A Conjugated Polymer Plastic Gel

by

Daniel Alcazar Jorba

SUBMITTED TO THE DEPARTMENT OF MATERIALS SCIENCE AND ENGINEERING IN PARTIAL FULFILLMENT OF THE REQUIREMENTS FOR THE DEGREE OF

MASTER OF SCIENCE IN MATERIALS SCIENCE AND ENGINEERING
AT THE
MASSACHUSETTS INSTITUTE OF TECHNOLOGY

SEPTEMBER 2008

Author .....
Department of Materials Science and Engineering
August 28, 2008

Certified by .....
Edwin L. Thomas
Head of the Department
Morris Cohen Professor of Materials Science and Engineering
Thesis Supervisor

Accepted by .....
Samuel M. Allen
POSCO Professor of Physical Metallurgy
Chair, Departmental Committee on Graduate Students

A Conjugated Polymer Plastic Gel

by

Daniel Alcazar Jorba

Submitted to the Department of Materials Science and Engineering
on August 28, 2008, in partial fulfillment of the requirements for the degree of
MASTER OF SCIENCE IN MATERIALS SCIENCE AND ENGINEERING

Abstract

We present a gel route to process highly oriented conjugated polymer films and fibers. The incorporation of hexafluoroisopropanol, a strong and stable dipolar group, to the polythiophene backbone enhances the solubility and especially, the hydrogen bond forming capabilities of the polymer. This functionalization enables the polymer to build up an isotropic self-supporting network structure based on a combination of polymer-polymer chain interactions and interchain hydrogen-bondings. These thermally reversible physical crosslinks incorporate plasticity in the conjugated polymer gel. The gel network can be melted and then transformed via mechanical deformation to form an anisotropic gel with the chains highly aligned along the tensile direction. The oriented gel morphology comprises a distribution of crystalline clusters in an overall swollen network. In these ordered regions, conjugated backbones are π-stacked with respect to each other neighbors. The mechanically induced structural rearrangement from an isotropic to an anisotropic conjugated polymer gel occurs when transitioning from the molten state to the gel state. This study highlights the versatility of incorporating plasticity in the design of conjugated polymer materials via a gel processing technology and its potential for applications.

Thesis Supervisor: Edwin L. Thomas

Title: Morris Cohen Professor of Materials Science and Engineering

Acknowledgements

First, I would like to express my deepest gratitude to my research advisor Prof. Edwin Thomas for his enthusiastic support and mentoring, his insightful suggestions and his patience and care throughout the preparation of this thesis. Ned has been central in the development of my scientific ability, teaching me to think more critically and to approach research in a more effective manner.

This research project was possible thanks to the innovative polymer chemistry of Prof. Timothy Swager in Department of Chemistry at MIT. I would like to gratefully acknowledge Prof. Swager's great generosity in sharing his knowledge and resources. I am also very grateful to Prof. Samuel Allen for guiding my academic progress at MIT during the past two years.

I'd like to thank my teammates and collaborators, in particular Steven Kooi, Vahik Krikorian, Henry Koh, Joe Walish, Raf Mickiewicz, Ji-Hyun Jang, Wei Zhang and Rebekah Bjork for creating a stimulating and supportive environment. Special thanks go to Fei Wang for preparing the polymer at the center of this research and for her assistance during my time at the chemistry laboratory and to Scott Speakman for his help in the x-ray diffraction part of this work.

Finally, my deepest feelings are to my family, especially to my parents. They made many sacrifices to give me the best opportunities possible. I'll always be thankful to them for instilling values of a good education and hard work.

Contents

List of Figures

List of Tables

Chapter 1

Introduction

1.1 Motivation

As conjugated polymer materials become available for commercial applications, there is a clear need to understand and improve their processing characteristics. A variety of technologies have been suggested depending on the approach chosen to overcome the typical infusibility and low solubility of unsubstituted conjugated backbones. The incorporation of side chains has become a common strategy to make otherwise intractable backbones processable. In the case of crystallizable conjugated polymers, the nature of these lateral pendant groups influences polymer morphology, optical and charge transport properties.

Conjugated polymers are appropriate for applications driven by large area, flexibility and low-cost. Of the technologies promoted, solution processing turned out to be the technique of choice for thin film deposition due to its low-cost and high-speed.[1] Nevertheless there exist drawbacks that seem difficult to address as they are inherent to the physical characteristics of this process. Solution processing consists on transitioning from a dilute polymer solution to a solid film via solvent evaporation. This type of process is appropriate for amorphous flexible chain polymers such as poly(methyl methacrylate). However, the situation for crystalline polymers is more challenging. Although good uniformities are obtained with regard to film coverage and thickness using spin-coating or spray-coating, the finite length of the polymer chains and the multiplicity of nucleation events results in inhomogeneous polycrystalline morphologies and poor control over the alignment of chains. The situation becomes even more challenging for crystalline rigid-rod polymers. Moreover, in multilayer architectures the solvents used for one layer can affect previously applied layers and limit the flexibility in device design.

In certain applications, anisotropic electronic and optical properties are of interest. In these situations, morphologies with uniaxially oriented chains can take advantage of the intrinsic anisotropy of the conjugated system along the chain axis. Furthermore, in materials design for electronic devices, the temperature is a relevant factor due to the viscoelastic nature of polymers. In this context, we suggest an ideal structure consisting on a three-dimensional network with uniaxial orientation of the

conjugated backbones in a continuous single crystal-like morphology. Our starting point relies on the synergistic combination of polymer gelation with mechanical orientation as a beneficial interplay between intermolecular interactions and ordering fields.[2] As an example, the work by Thomas and Cohen demonstrated the formation of a crystal-solvate phase between a molecularly stiff polymer and its solvent during the coagulation stage of fiber spinning resulting in high degree of crystallinity and uniaxial alignment of the chains.[3]

This thesis constitutes an exploratory study of a novel gel processing route to incorporate plasticity in conjugated polymers. The polymer at the center of this research is a dipole functionalized polythiophene prepared by Professor Swager's group in Department of Chemistry at MIT. The chemical nature of the hexafluoroisopropanol (HFIP) pendant group results in a periodic incorporation of hydroxyl moieties along the backbone able to participate in strong hydrogen bonding associations. The approach followed is based on a two step strategy, first gelation of hexafluoroisopropanol functionalized polythiophene (HFIP-PT) with small polar protic molecules, essentially poor solvents/non-solvents. The gelation mechanism likely combines polymer-polymer chain interactions and interchain associations promoted by hydrogen bonding. Second, melting the gel network followed by mechanical processing into films and fibers with uniaxial orientation of the chains along the tensile direction.

1.2 Thesis Overview

The general framework of this study is presented in Chapter 2. Starting with an introductory overview on the semiconducting nature and charge transport properties of conjugated polymers, we then discuss solution processing of crystallizable regioregular polythiophenes with a particular emphasis on the relationship between structure, morphology and electronic properties. As a source of inspiration and to illustrate the actual need for this type of research, we review the major techniques proposed to date to engineer chain alignment in conjugated polymer materials.

In Chapter 3, we report the detailed procedure followed to prepare HFIP-PT gels. The gelation mechanism is analyzed by means of Fourier transform infrared spectroscopy. We suggest HFIP-PT is able to build up an isotropic self-supporting network structure based on a combination of chain-chain polymer interactions and interchain associations between HFIP pendant groups through hydrogen bonding with small polar protic molecules such as methanol and water.

The method to prepare the oriented gel films and the techniques used for structural analysis (light and electron microscopy and electron and x-ray diffraction) are presented in Chapter 4. The degree of in plane chain alignment is further quantified by dichroism analysis. Based on optical and diffraction analyses, we propose an oriented gel morphology consisting in an anisotropic distribution of paracrystalline clusters in an overall swollen network. In these ordered phases,

HFIP-PT chains are highly aligned and π-stacked with respect to one another. The ability of the gel to attain highly anisotropic morphologies upon mechanical orientation during the reformation transition from the molten state to the gel state is attributed to the rigidity of polythiophene backbones and stress transmission through a network of linkages based on chain-chain interactions and hydrogen bonding associations.

The impact of the high stress fields that build up during fiber spinning became apparent upon preparation of oriented gel fibers. A significant degree of structural anisotropy appeared in necked regions of the fibers. The methodology to pull fibers and their structural characterization are presented in Chapter 5.

Over the course of this study, we went from exploring to realizing the potential of a plastic gel route to process conjugated polymers. Although many aspects of this approach are still in a preliminary stage of understanding, the findings suggest that there is a new worthwhile potential platform to design and process conjugated polymer materials. The most relevant insights of this research and our suggestions for future work are summarized in Chapter 6.

Chapter 2

Background

In recent years, there has been an increased interest in using conjugated polymer materials for commercial uses. Fundamental properties like electrical conductivity and electroluminescence along with the potential for further functionalization allows conjugated polymers to be competitive candidates for transistors, sensors and light-emitting diodes.[4] In this chapter, we give an overview of this type of polymeric material with a particular emphasis on processing, structure and charge transport properties of polythiophenes (PT's)[5] and review representative approaches to attain morphologies with uniaxial alignment of chains for conjugated polymers in general.

2.1 Introduction to Conjugated Polymers

A variety of synthetic strategies and chemical structures have been explored to prepare conjugated polymers, driven by the interest to improve processability, stability and interfacial interactions in devices and the possibility to chemically enhance and tailor properties. Figure 2-1 shows a set of representative conjugated polymers; all their chemical structures are based on a macromolecular backbone with alternation of single and double bonds resulting in a conjugated system of π-electrons. The energy difference between the highest occupied molecular orbital (HOMO) and the lowest unoccupied molecular orbital (LUMO) in conjugated molecules becomes a band gap as the length of the conjugated sequence increases. As the number of interacting orbitals increases in a conjugated system, the HOMO shifts to higher energy levels and the LUMO to lower energy levels which results in a decrease in band gap energy (E_g). Depending on the magnitude of E_g, conjugated polymers can exhibit semiconducting properties and become the functional materials in light-emitting diodes, electrochromic devices and photovoltaic cells. The bandgap can be tuned via changes in the chemical structure of the backbone or by systematically changing the type of substituent in a particular family of conjugated polymers.

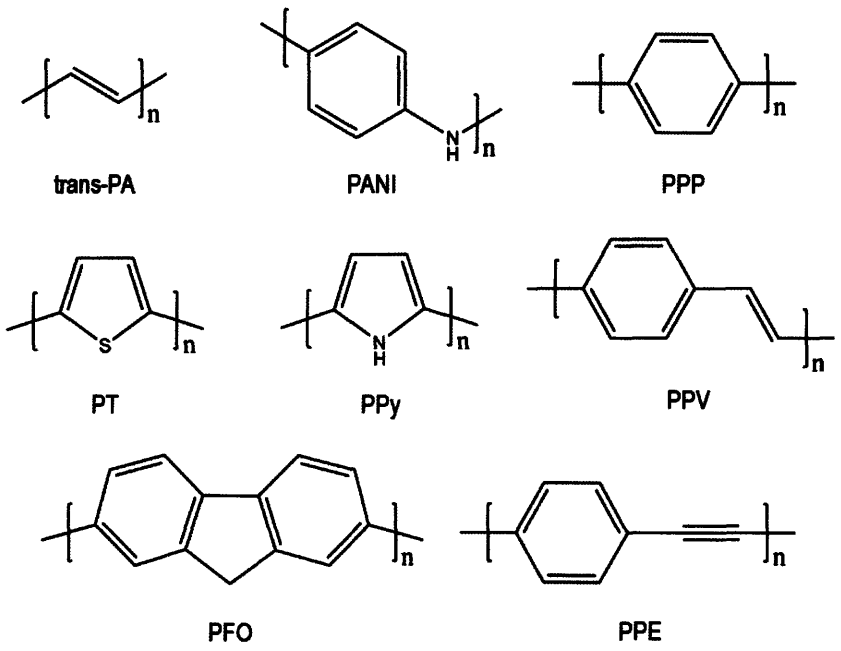

Figure 2-1. Chemical structures of important conjugated polymers: Trans-polyacetylene (trans-PA), polyaniline (PANI), poly(p-phenylene) (PPP), polythiophene (PT), polypyrrole (PPy), poly(phenylene vinylene) (PPV), polyfluorene (PFO) and poly(p-phenylene ethynylene) (PPE). Reproduced from Ref. [4].

In the neutral form, conjugated polymers are either insulating or semiconducting materials. In a seminal contribution, Shirakawa et al. showed that conductivity (σ) can change by orders of magnitude from the neutral to the doped state in polyacetylene (PA) films.[6] Naarmann and Theophilou further optimized film preparation and reported an increase in conductivity of trans-PA films from 10^{-5} Scm^{-1} to $1.6x10^{4}Scm^{-1}$ upon doping and up to $10^{5}Scm^{-1}$ upon doping and further film

stretching (I_2 doped and draw ratio (λ) of 5),[7] a magnitude comparable with that of metals (copper has a conductivity of $5.9x10^5 Scm^{-1}$ at 20°C).[8] Doping in conjugated polymers can be achieved by oxidation or reduction reactions which form delocalized charge carriers. Oxidative doping (p-doping) is more stable than reductive doping (n-doping) because anionic polymers easily react with oxygen or water.

As a result of coupling to chain distortions, the charges introduced through doping are in states that include a charge and a lattice distortion. In structures with a degenerate ground state such as PA, charges are stored in states regarded as solitons which can be illustrated by bond alternation domain walls along the chain. In systems with a non-degenerated ground state like polyheterocycles such as PT's, the quinoid form has a higher energy than the benzoid form and polarons and bipolarons turn out to be the charge storage configurations. Polarons are described as a charged soliton bound to a neutral soliton due to confinement. Bipolarons in turn can be described in simple terms as a confined pair of charged solitons.[9] Figure 2-2 illustrates these charge storing configurations on the chemical structures of trans-PA (degenerate) and PT (non-degenerate).

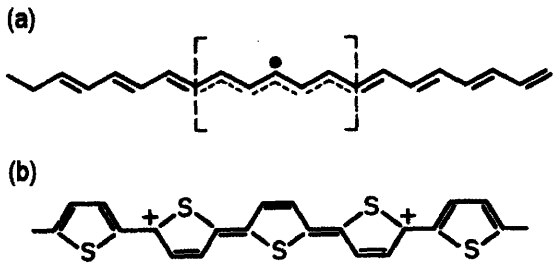

Figure 2-2. (a) Neutral soliton in PA, (b) Doubly charged bipolaron in PT. Reproduced from Ref. [9].

Although high conductivities can be attained, in general conjugated polymers present lower values compared to inorganic semiconductors. This difference is explained in terms of a lower concentration of charge carriers and a lower mobility. The lower level of charge carrier density is attributed to a poor degree of compositional uniformity during doping. The lower mobility is thought to be the consequence of a higher presence of impurities, chemical defects and structural disorder.[10] Impurities refer to unwanted chemical species, from solvents to contaminants, while chemical defects denote imperfections in the molecular structure arising from side reactions like chain-branches or stochastic reactions such as those affecting the regiochemistry of the polymer. Impurities and chemical defects are considered to be the principal sources of localized energy levels, so called traps, where charge carriers can be immobilized. Structural disorder refers to those aspects in the morphology of conjugated polymers that limit the propagation

of charge carriers from the source to the drain electrodes, i.e. amorphous regions, crystal-amorphous interfaces and a random distribution of chain axes. Moreover, due to the finite length of polymer chains, macroscopic transport requires charge carriers to hop or diffuse from one chain to another even in well ordered regions. In a study on the anisotropic conductivity in oriented PA films, Wang et al. suggested that in those regions where chains can adopt a parallel crystalline packing, electron waves could extend along several chains in three-dimensions.[11]

The ability to improve conductivity upon film stretching revealed the importance of microstructure in the electronic properties of conjugated polymers. As illustrated by the work of Fincher et al. on stretched PA films, anisotropic reflectance analysis indicated a high degree of chain alignment along the stretching direction. In the same study, optical anisotropy was found to increase upon doping (I_2 or AsF_5).[12] Similarly, conductivity measurements in stretched PA films showed higher values when measured along the chain axis compared to measurements done perpendicularly. Cao et al. reported a linear increase in parallel conductivity with draw ratio in oriented PA films while the conductivity perpendicular to the tensile drawing direction was essentially constant for $\lambda \geq 2$. At a draw ratio approaching 15, the anisotropy increased up to $\sigma_{\parallel}/\sigma_{\perp} \sim 250$ as illustrated in Figure 2-3.[13]

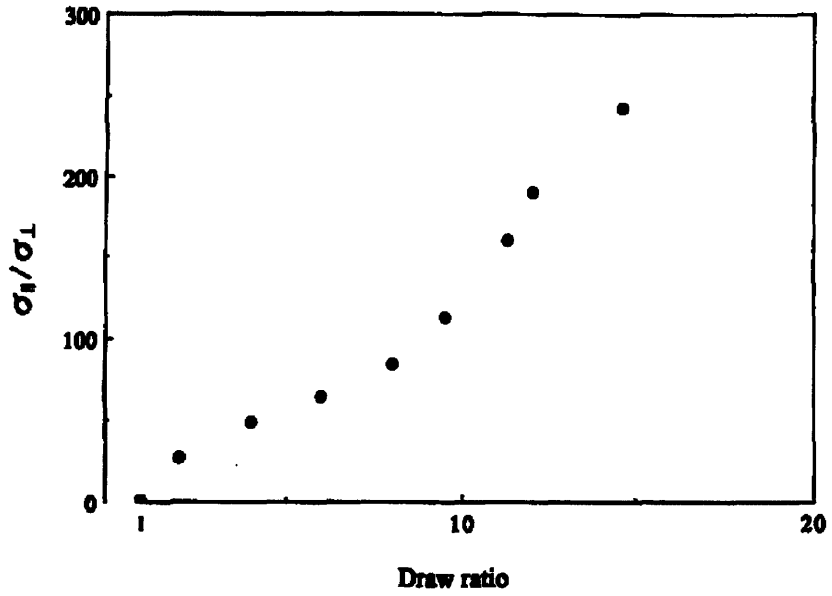

Figure 2-3. Anisotropy of the electrical conductivity dependence with draw ratio in oriented PA films. Reproduced from Ref. [13].

2.2 Morphology and Charge Transport in Polythiophenes

The synthetic versatility and excellent thermal and environmental stability of PT's has motivated the exploration of a wide variety of chemical structures.[14] Thermal and environmental degradation accounts for the deterioration of the polymer chemical structure due to factors such as temperature, light, oxygen and

moisture among others. In a closed, dry and oxygen-free environment, degradation mechanisms are referred to as intrinsic. Under these conditions, the initiation of chemical reactions is attributed to charged sites along the polymer chain and to dopant counterions. A critical consequence of either extrinsic or intrinsic degradation mechanisms is the introduction of saturated defects (sp^3 hybridized carbons) breaking the conjugated system along the chain. The stabilities of PT's are half-way between that of PA, which is considered as unstable, and polypyrroles (PPy's) which are among the most stable conjugated polymers.[15] Rubner and coworkers conducted a systematic study of thermal and environmental stability in poly(3-alkylthiophenes) (P3AT's). It was found that stability increases as the side-chain length decreases, that it strongly depends on the type of doping process and to a lesser extent on the type of polymerization method. As an example, the electrical conductivity in $FeCl_3$ doped poly(3-hexylthiophene) (P3HT) decayed by one order of magnitude after 17,000min at 80°C in dry nitrogen.[16]

Doping in PT's is usually conducted by direct exposure to chemical dopants. Films are immersed in a solution (e.g. $FeCl_3$ in nitromethane) or enclosed under saturated environment (e.g. I_2 or Br_2 vapors). However, iodine and bromine can more easily evaporate resulting in faster de-doping compared to $FeCl_3$.[17] Although p-doped conjugated polymers are known to be more stable than n-doped, the addition of electron withdrawing pendant groups, such as perfluoroalkyls, has been explored as a route towards more stable n-dopable PT's.[18]

Unsubstituted PT results in infusible materials with very low solubility; molecular weights higher than 3kD are even insoluble in hot chloroform.[19] The incorporation of lateral pendant groups in polythiophenes has become a common strategy to make these otherwise intractable materials processable.[20] As illustrated in Figure 2-4, the regiochemistry of 3-substituted polythiophene derivatives depends on the sequence of linkages between monomers. In general, regioregularity accounts for the type of arrangement of the monomer units during polymerization. Regioselective polymerization will favor one type of arrangement, head-to-tail (HT), head-to-head (HH) or tail-to-tail (TT).[21]

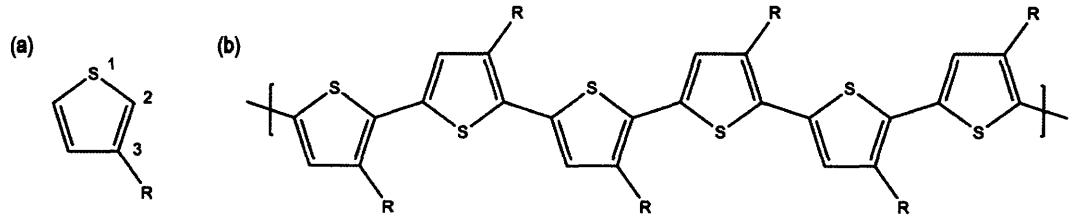

Figure 2-4. (a) Chemical structure of a 3-substituted thiophene derivative. The incorporation of a functional group in position 3 yields a monomer with lower symmetry. (b) A regioregular heat-to-tail 3-substituted polythiophene. A sequence of 6 monomers is depicted to visualize the molecular regularity along the backbone.

Regiorandom P3AT's result in higher steric interactions between the alkyl groups compared to the regioregular H-T configuration. Steric hindrance between

pendant groups can force neighboring thiophene rings out of a 180° dihedral angle with respect to each other which results in a loss of backbone planarity and reduction of the conjugation length.[22] The polymer band gap decreases as the extent of conjugation increases and this is directly reflected in the maximum wavelength of absorption in the ultraviolet-visible (UV-VIS) spectrum.[23] The variation in conjugation length from regiorandom to HT regioregular P3AT's has been quantified in terms of a red-shift of the maximum absorption peak,[24] see Figure 2-5. The addition of enantiomerically pure side groups can induce a handed twist of the backbone in 3-substituted regioregular PT. Bouman and Meijer reported on circular dichroism analysis of regioregular (98% HT) 3-[2-((S)-2-methylbutoxy)ethyl]-substituted polythiophene films showing an optical activity that was attributed to the presence of chiral helical structures.[25]

In asymmetrically substituted polythiophenes, the degree of regioregularity plays an important role in molecular packing and crystallization. Higher regioregularity favors a better molecular registry enabling the formation of regions with an ordered packing of chains, in analogy with stereoregular polymers.[26] Thin films of P3AT with higher degree of regioregularity present better electrical conductivity compared to the regiorandom counterparts. McCullough and Lowe found that higher regioregularity results in enhanced electrical conductivity. For example, the conductivity of iodine doped poly(3-dodecylthiophene) solution cast

films increased by a factor of 60 times from 10 Scm^{-1} for regiorandom (54% H-T) to 600 Scm^{-1} for regioregular (91% H-T) configurations.[27]

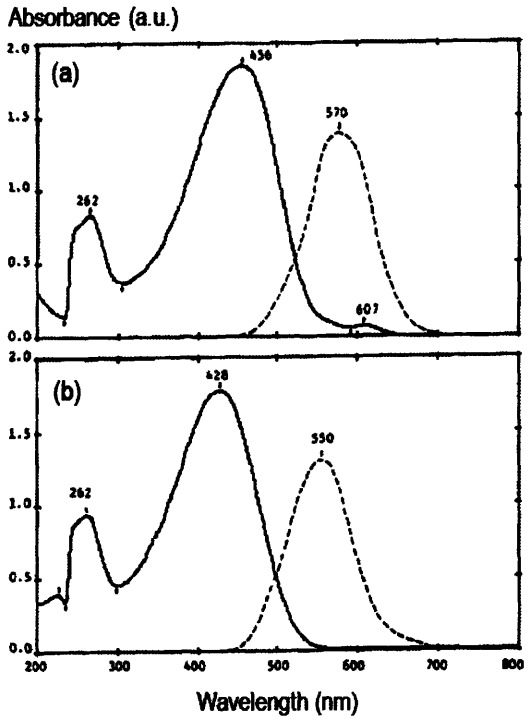

Figure 2-5. UV-VIS (solid line) and fluorescence (dashed line) spectra of (a) regioregular P3HT with HT coupling >98.5% and (b) regiorandom P3HT with 50/50 HT/HH couplings in chloroform solution. The shift of the maximum absorption peak corresponds to an energy reduction of 0.2eV from regiorandom to regioregular configurations. Reproduced from Ref. [24].

The effect of morphology on charge transport is particularly apparent in thin film transistors based on solution processable polythiophenes.[28] Their

performance is usually benchmarked against amorphous silicon with a charge carrier mobility of 0.5-1$cm^2V^{-1}s^{-1}$. For a thin film made by solution casting, the polymer undergoes a drastic change in its physical state.[29] Solution processing comprises transitioning from a dilute polymer solution to a solid film via solvent evaporation. Although good uniformities are obtained with regard to film coverage and thickness using spin-coating or spray-coating, the finite length of polymer chains and the multiplicity of nucleation events results in inhomogeneous polycrystalline morphologies and poor control over the alignment of chains. As it is often encountered in most crystallizable polymers, the solvent cast film morphology generally contains a mixture of lamellar crystallites and amorphous interlamellar regions. Inside the lamella, the conjugated chains are π-stacked with respect to one another and their axes lie approximately normal to the plane of the platelet and in thin films parallel to the substrate. In plane π-stacking of backbones results in strong polymer-polymer chain interactions.

Several factors need to be taken into account when analyzing charge transport properties in solution deposited conjugated polymer thin films. Solvent, density of molecular defects, thermal treatment, polymer molecular weight, degree of regioregularity and nature and concentration of dopant all are critical features in determining charge transport. The charge carrier mobility in thin films of P3HT is known to increase with higher degree of regioregularity and molecular weight. As an example of the impact of regioregularity, Figure 2-6 illustrates the increase in

mobility with degree of regioregularity in thin films of P3HT cast from chloroform solution.[30]

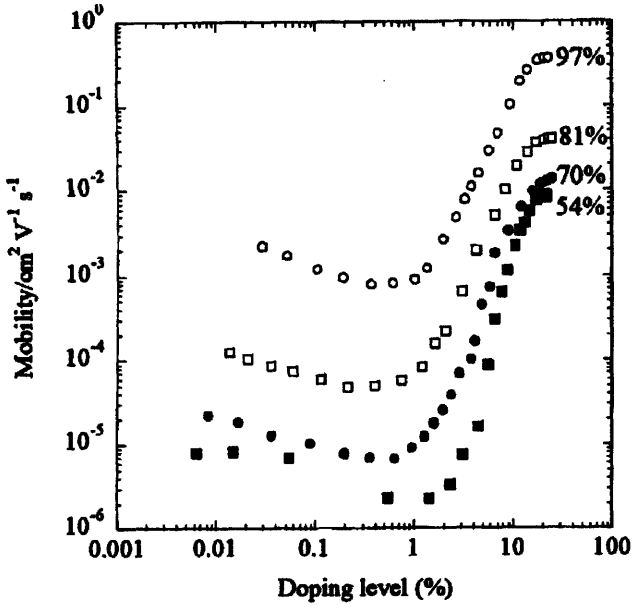

Figure 2-6. Charge carrier mobility dependence on degree of regioregularity and doping level in thin films of P3HT. Reproduced from Ref. [30].

With regard to molecular weight dependence, McGehee and collaborators reported an increment in charge carrier mobility from $1.7x10^{-6}cm^2V^{-1}s^{-1}$ to $9.4x10^{-3}$ $cm^2V^{-1}s^{-1}$ for molecular weights of 3.2kD and 36.5kD respectively in thin films of regioregular P3HT spin cast from chloroform solutions.[31] In this study, higher mobilities were reported for higher molecular weights even though low molecular

weight samples presented a higher degree of crystallinity (The intensity of the (100) peak on the x-ray diffractogram was used to quantify the degree of crystallinity). Figure 2-7 illustrates the surface morphologies of 3.2kD and 31.1kD P3HT films from the same study. This polycrystalline morphology contains thin (~10 nm) platelet-like crystallites limited to a few microns in lateral area which results in a high density of crystal-amorphous boundaries. The presence of crystal-amorphous interfaces seems to be a limiting factor for charge transport. While inside the lamella chains are well-ordered, amorphous regions usually contain randomly distributed chains or chain termination segments; Figure 2-10 illustrates some of these concepts, the red lines seem to indicate three main features, chain folding which seems reasonable given the size of the lamellar domains and the molecular weight of the polymer, connective chains between crystalline domains and chain termination. However, the red lines seem a little too bent in some cases. In our HFIP-PT gel morphology drawing in Figure 4-9, we illustrate the less densely packed regions in between ordered cluster using more straight lines to represent stiff backbones. The gain in mobility found for higher P3HT molecular weights was attributed to less well defined boundaries compared to low molecular weight counterparts and to the presence of longer chains that may act as connective transport pathways between well ordered domains in higher molecular weights samples.

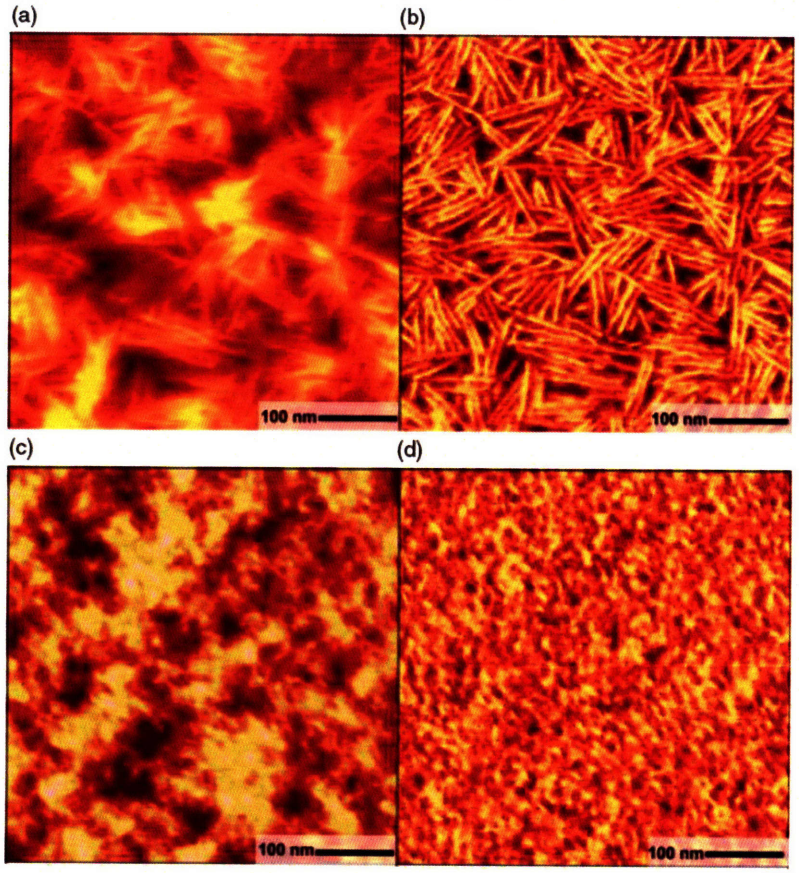

Figure 2-7. Tapping mode atomic force microscopy of regioregular P3HT thin films. Films were spin cast from chloroform solution. (a) and (b) height contrast (topography) and phase contrast (stiffness) respectively for a 3.2kD molecular weight. (c) and (d) height and phase contrast respectively for a 31.1kD molecular weight. Reproduced from Ref. [31].

Model PT oligomers are a useful starting point to review the structural analysis of this family of conjugated polymers at the molecular level.[32] Complete structural studies of single crystals of unsubstituted α-nT have been reported up to

the octamer (α-nT, α indicates the type of linkage sequence between thiophene units which corresponds to the one depicted in Figure 2-4 and n represents the number of thiophene units). A herringbone mode of packing is generally found in unsubstituted α-nT oligomers. In this mode of arrangement, molecules pack with the long axis of the molecule in a parallel fashion and with 40°-60° dihedral angles between molecular planes. As an example, the work by Horowitz et al. shows this type of herringbone arrangement in the unit cell structure of α-6T single crystals as grown from the vapor phase.[33] The origin of the herringbone arrangement in oligothiophenes is attributed to the repulsion between π-orbitals in neighboring molecules. This particular packing mode is expected to reduce the charge transport efficiency in the direction normal to the long molecular axis. This type of packing mode observed in α-nT oligomers has also been found in unsubstituted PT. Brückner and Porzio reported on the x-ray diffraction analysis of chemically synthesized PT powders. Based on 11 reflections, their analysis showed a structure that follows a herringbone mode of arrangement as illustrated in Figure 2-8.[34]

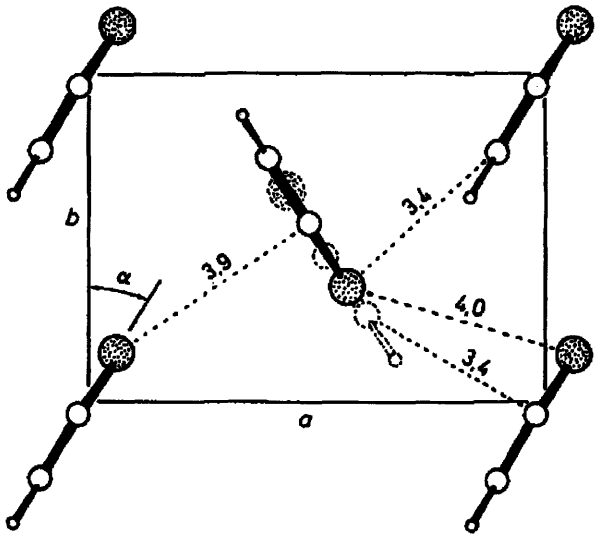

Figure 2-8. Structure of the a-b plane orthogonal to the chain axis of PT. Interchain distances are reported in Angstroms. Reproduced from Ref. [34].

A successful strategy to get the desired π-stacking configuration is to attach substitutional groups that can force conjugated oligomers and polymers to adopt face to face stacking of backbones instead of a herringbone mode of packing. The work of Prosa et al. on the structural analysis of hexyl, octyl and dodecyl-substituted PT's suggested the presence of lamellar structures with stacks of planar PT chains spaced by alkyl chains.[35] The general structure proposed for regioregular P3AT is illustrated in Figure 2-9.

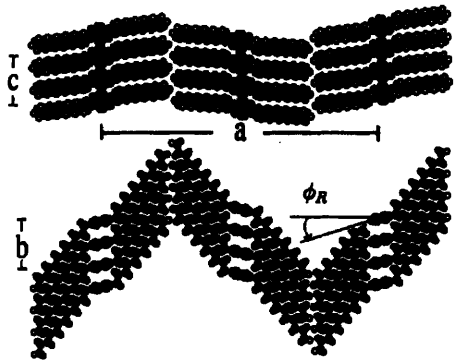

Figure 2-9. General structural arrangement proposed for P3AT based on a parallel stacking of backbones along the b-axis. Reproduced from Ref. [35].

A recent study on oriented thin films prepared by directional eutectic solidification is an illustrative work to visualize the relationship between the lamellar type of morphology and the structure at the molecular level in regioregular P3HT. Directional eutectic solidification consists of two major steps, first the polymer forms a dilute solution with a *crystallizable* solvent and second the liquid eutectic mixture is cooled under a temperature gradient. Upon cooling, the solvent and polymer segregate, the polymer chains aggregate and then epitaxially crystallize on the surface of the previously directionally crystallized solvent. As illustrated in Figure 2-10, directional solidification of P3HT on 1,3,5-trichlorobenzene results in thin films with an edge-on configuration of the lamellae. In the molecular analysis of the lamellar morphology, Brinkmann and Wittmann reported a structure based on an arrangement of P3HT chains lying parallel to the bc plane, an edge-on orientation

of the backbones stacked along the b-axis and an interdigitation of the pendant alkyl groups.[36]

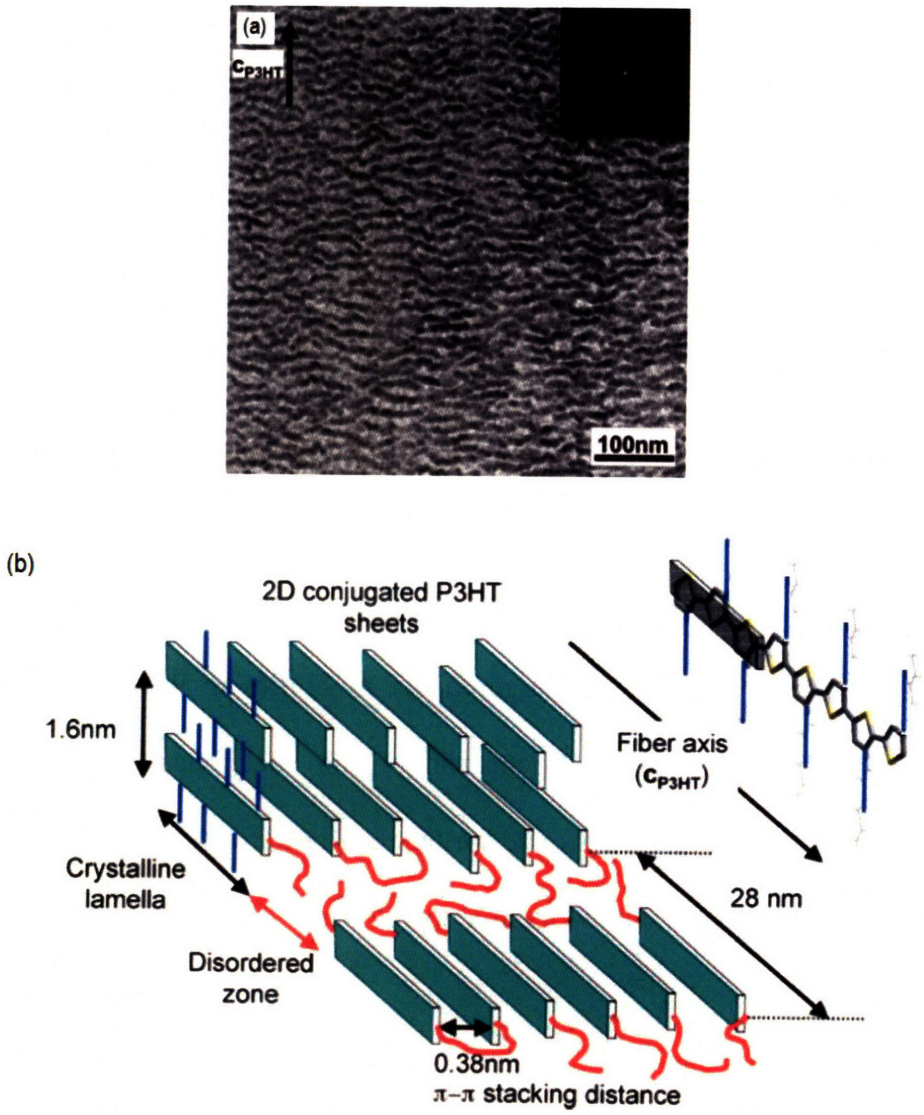

Figure 2-10. (a) Bright-field transmission electron micrograph of a P3HT thin film grown by directional eutectic solidification. The dark strips correspond to lamellar

structures, they are oriented edge-on with respect to the substrate. The arrow indicates the direction of the P3HT chain axis (c_{P3HT}), it is normal to the long direction of the lamellae in the micrograph. The inset corresponds to the fast Fourier transform of the image, the reflections correspond to the first order of the lamellar structure with a periodicity of 28nm. (b) Schematic of the arrangement of the chains inside the lamellar structure. P3HT chains lie parallel to the substrate and with an edge-on orientation of the backbones. The drawing also illustrates the interdigitation of the lateral pendant alkyl groups. Reproduced from Ref. [36].

The relative orientation of the backbones with respect to the substrate is thought to be relevant in charge transport efficiency. The two extreme orientations, namely face-on and edge-on, correspond to the plane of the conjugated backbone parallel and perpendicular to the substrate respectively, see Figure 2-11. The transport between source and drain electrodes takes place along the plane of the conjugated polymer film. High charge carrier mobilities in P3HT thin films have been attributed to an edge-on orientation of the backbones. Sirringhaus et al. suggested that the high mobility found for this configuration arose from the bc plane forming a two-dimensional π-electron plane due to the overlap of electron wavefunctions.[37]

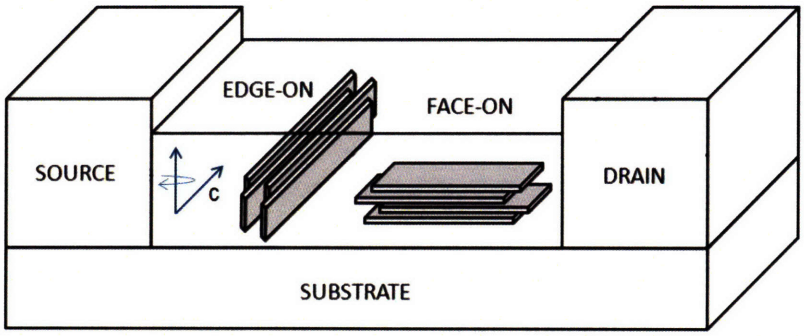

Figure 2-11. Edge-on and face-on orientations of conjugated backbones and their relative arrangement with respect to the source and drain electrodes in a typical thin film device architecture with planar isotropic texture. Dimensions are not to scale.

The interaction between the conjugated polymer and the dielectric surface has been investigated due to the relevant role of thin film microstructure close to that interface in field effect transistors.[38] Depending on the type of functional group present at the dielectric surface it is possible to selectively induce face-on or edge-on orientation of the backbones during thin film deposition. Kim et al. showed that on surfaces modified with NH_2 groups P3HT films present a preferentially edge-on orientation of the chains with a mobility of $0.28 cm^2V^{-1}s^{-1}$, higher when compared to $0.08 cm^2V^{-1}s^{-1}$ obtained for films with face-on orientation prepared on surfaces grafted with CH_3 groups.[39]

2.3 Engineering Chain Alignment in Conjugated Polymers

The arrangement of polymer chains with respect to the electrodes, the volume fraction of amorphous regions and the density of crystal-amorphous interfaces are relevant structural factors in crystallizable conjugated polymer thin films affecting charge transport and optical properties. Chain alignment, in particular, can result in enhanced anisotropic conductivity and optical anisotropy such as polarized luminescence or absorbance. Several techniques have been proposed to overcome isotropic polycrystalline morphologies which contain numerous interfaces/amorphous regions and take advantage of the intrinsic anisotropic nature of the individual conjugated polymer chains.

These approaches include:

(1) Processing rigid chain-flexible chain binary blends with ultra high molecular weight polyethylene was promoted by Andreatta and Smith to prepare uniaxially oriented polyaniline films.[40]

Based on a similar approach, Montali et al. processed ternary blends of ultra high molecular weight polyethylene, a poly(2,5-dialkoxy-p-phenylene ethylene) derivative and a sensitizer into uniaxially

oriented films with an isotropic absorption of light but emission in highly polarized fashion.[41]

(2) Epitaxy has been a useful tool for the structural analysis of crystalline polymers as illustrated by the work of Wittmann and Lotz.[42] It has also been proposed as a route towards preparing highly oriented films of organic materials.[43] In the case of polydiacetylenes, a monomer film deposited by sublimation onto an alkali halide substrate can be later polymerized preserving its epitaxial orientation (epipolymerization).[44]

(3) Alignment on rubbed polymer films has been proposed to orient conjugated polymers following the established technique for liquid-crystal phases. Grell et al. prepared highly oriented liquid-crystalline polyfluorene (PFO) derivatives films by solution-casting onto mechanically rubbed polyimide (PI) substrates.[45] In a similar approach, Sakamoto et al. used photoaligned PI substrates to orient the liquid-crystal rigid chain-solvent phases.[46]

Kanetake et al. reported on the solid state photopolymerization of diacetylene monomers conducted on rubbed layers of polyesters[47] or polydiacetylene.[48]

(4) Rubbing has been directly applied to conjugated polymer films to induce chain alignment. Hamaguchi and Yoshino showed polarized light emission from a poly(phenylenevinylene) film after rubbing a previously spin coated film with a suitable tissue in a single direction to impart uniaxial orientation.[49]

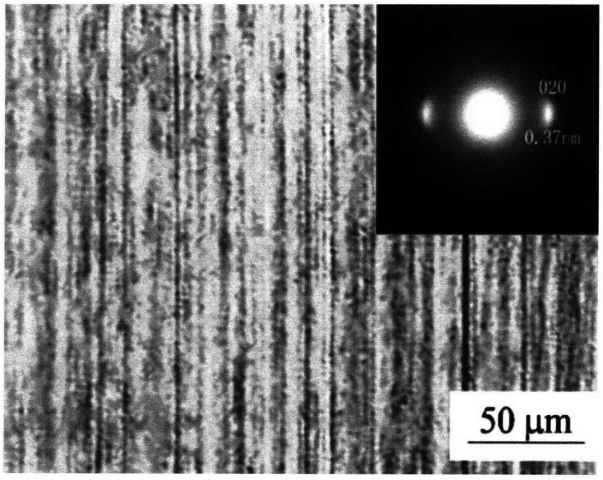

Figure 2-12. Polarized light micrograph showing the birefringence of a rubbing aligned regioregular P3HT thin film. The inset corresponds to the transmission electron diffraction pattern of the film. The strong equatorial reflections indicates that chains are stacked along the b-axis. Reproduced from Ref. [50].

Yang et al. obtained aligned regioregular P3HT morphologies upon rubbing a thin film with the smooth edge of a quartz slide. As

illustrated in Figure 2-12, polarized light microscopy and electron diffraction indicated that the c-axis was aligned mostly along the rubbing direction and that both c-axis and b-axis were parallel to the plane of the film.[50]

(5) Langmuir-Blodgett techniques combine the possibility to control the thickness of the conjugated polymer film on the liquid surface with the ability to induce a preferential orientation of backbones along the dipping direction during film transfer onto a substrate. Cimrova et al. found a significant degree of optical anisotropy in Langmuir-Blodgett iso-pentoxy substituted poly(p-phenylene) films as illustrated in Figure 2-13.[51]

(6) Uniaxial stretching has been applied on a variety of conjugated polymers films and in combination with other techniques such as processing of blends as illustrated in point (1). Cao et al. reported on the electrical properties of oriented PA films. Tensile drawing resulted in a linear increase in conductivity with the draw ratio. At a draw ratio approaching 15, the anisotropy increased up to $\sigma_{\parallel}/\sigma_{\perp} \sim 250$.[52]

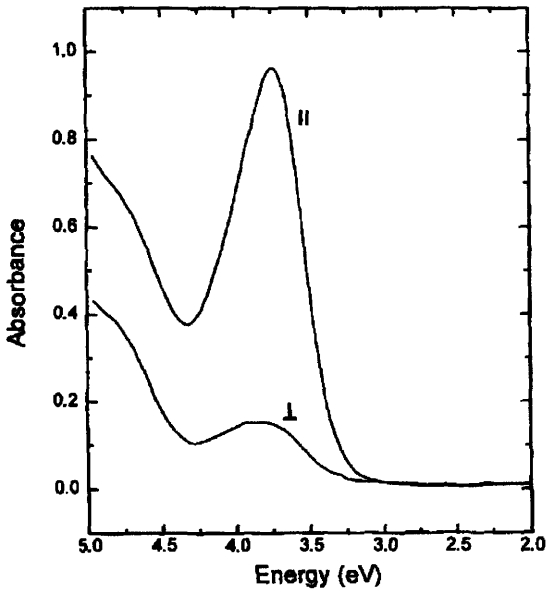

Figure 2-13. Absorption spectra corresponding to an iso-pentoxy substituted poly(p-phenylene) film prepared via a Langmuir-Blodgett technique. The optical anisotropy of the thin film is illustrated by the difference between the parallel and normal spectra (directions refer to the dipping direction). Reproduced from Ref. [51].

Polarized emission has been reported from stretch-oriented poly(3-(4-octylphenyl)-2,2'-bithiophene) films. The intensity ratio between light emitted parallel and perpendicular to the chain axis was 2.4 after film was stretched to 200% of its original length.[53] A similar optical anisotropy was observed upon uniaxial stretching of electrochemically polymerized PT films.[54]

In a recent study from this group, Pytel et al. reported on the anisotropy in electroactive strain due to chain alignment in PPy films up to a factor of 38 between the strain parallel and normal to the chain axis. X-ray diffraction (XRD) analysis clearly showed the building of structural anisotropy upon degrees of elongation of 142%.[55]

(7) Block copolymer-rigid rod co-assembly under a bias field to induce uniaxial alignment of the guest. The Swager and Thomas groups showed how a styrene-isoprene-styrene triblock copolymer (host) self-assembled into a cylindrical morphology via the roll-casting method developed by Albalak and Thomas[56] can induce uniaxial alignment of the guest, a styrene grafted poly(p-phenylene-ethynylene). The styrenic functionalization introduced a selective miscibility of the conjugated polymer to the cylinder domains.[57]

(8) Soft-lithography combined with solventless polymerization in channels was reported by Gu et al. to produce oriented PA films. The process consists on selectively expose regions of a catalyst layer by using a channeled polydimethylsiloxane mask wherein polyacetylene films are prepared via solventless ring-opening methatesis polymerization upon exposure to monomer vapors.[58]

(9) Preferential orientation of chains along the long axis of the channels via embossing conjugated polymer films within the channels of a silicon mold. Hu et al. proposed a process applicable to conjugated polymers like PFO's, PT's and PPy's based on pressing a mold against a fluid polymer film followed by crystallization either by cooling or solvent evaporation.[59]

In a similar approach, Zheng et al. employed a silicon master to pattern nanolines on a PFO derivative film by letting the polymer flow into the channels at a temperature above its glass transition. After cooling, polarized absorption and photoluminescence indicated a preferential orientation of the chains parallel to the imprinted lines.[60]

(10) Friction transfer has been employed to align crystallizable polymers such as poly(tetrafluoroethylene) (PTFE) thin films.[61] The process consists on moving a poly(tetrafluoroethylene) bar against a smooth surface such as a glass slide, at a controlled rate, surface temperature and pressure. A similar friction-transfer technique has recently been used by Misaki et al. to form a highly oriented single crystal-like morphology of poly(9,9-dioctylfluorene) films.[62]

(11) Blending conjugated polymers into a nematic liquid crystal to increase polymer interchain interactions. Hydrogen-bonding extension

of the chain-end has been proposed as a route to induce anisotropic self-assembly through increased polymer interchain interactions. Hoogboom and Swager found a higher degree of chain alignment when blending a poly(phenylene ethynylene) derivative end capped with hydrogen bonded groups into a nematic liquid crystal.[63]

(12) Supramolecular assembly of conjugated polymers. Kubo et al. proposed a method consisting on functionalization of conjugated polymer with a suitable group to cooperatively interact with bundling molecules interleaving between chains, similar to a lego-type of assembly.[64]

(13) The soluble precursor polymer strategy has been used to prepare thin films of several conjugated polymers such as PA[65] or poly(phenylene vinylene) (PPV)[66]. In the later study, this approach resulted in highly aligned uniaxial film morphologies by simultaneously orientation and conversion of a soluble polyelectrolyte precursor. Figure 2-14 shows the electron diffraction of oriented PPV films at a draw ratio of 14. The features observed are indicative of a regular packing of PPV chains aligned along the drawing direction and the presence of axial translational disorder, a common feature found in biological structures as well as other synthetic polymers.

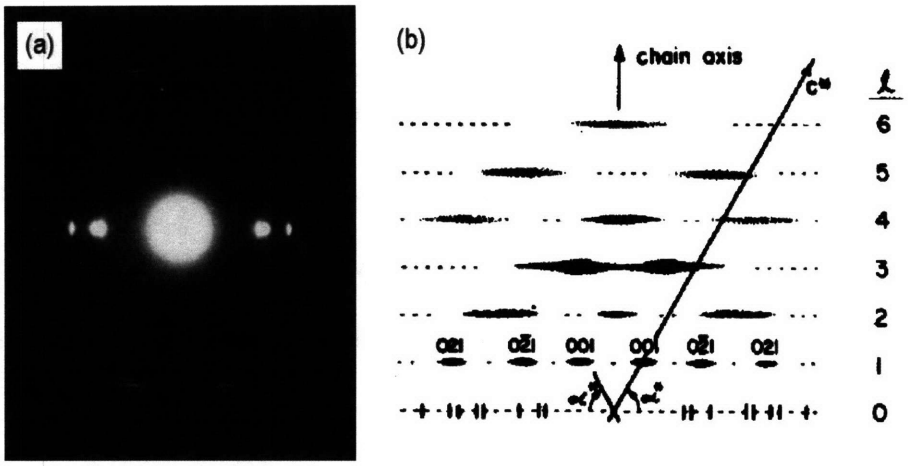

Figure 2-14. (a) Electron diffraction pattern of an oriented PPV film prepared via the soluble precursor polymer method. (b) Schematic of the diffraction pattern. Reproduced from Ref. [66].

(14) Directional eutectic solidification is a technique to direct the assembly of crystallizable polymers[67] as well as crystallizable block copolymers.[68] As described above the method has been applied to orient thin films of regioregular P3HT, see Figure 2-10.

The addition of lateral pendant groups to conjugated polymer backbones facilitates processing. In the case of crystallizable conjugated polymer, such as regioregular polythiophenes, solution deposition of thin films typically results in isotropic polycrystalline morphologies. However, certain applications can benefit from anisotropic charge transport and optical properties. The interest in developing

conjugated polymer materials with oriented morphologies has triggered the exploration of a variety of processing strategies toward chain alignment.

The properties of polymeric material can change upon addition of small molecules, inorganic materials and/or other polymers via blending. This is extensively used in plastics engineering where formulations usually contain additives to improve their processability and functionality. Gelation illustrates how the addition of new constituents introduces competing interactions able to tune the physical state of a polymer system.[69] Gel processing combined with uniaxial stretching shows a beneficial interplay between intermolecular interactions and ordering fields.

Chapter 3

Gelation of Hexafluoroisopropanol Functionalized Polythiophene

Section 3.1 describes the experimental work to prepare and characterize HFIP-PT gels, namely the materials, gelation protocol and analytical techniques. In Section 3.2, we propose a gelation mechanism based on nuclear magnetic resonance (NMR), Fourier transform infrared (FTIR) spectroscopy and light microscopy (LM) studies.

3.1 Procedure

3.1.1 Materials

HFIP-PT was prepared by Professor Swager's group in Department of Chemistry at MIT. The molecular structure of HFIP-PT, poly(3'-hexafluoroisopropanol-2,2':5',2''-terthiophene), is shown in Figure 3-1. HFIP is a strong hydrogen bond donor group often used in chemical sensing such as for the detection of phosphate esters common to chemical warfare agents.[70]

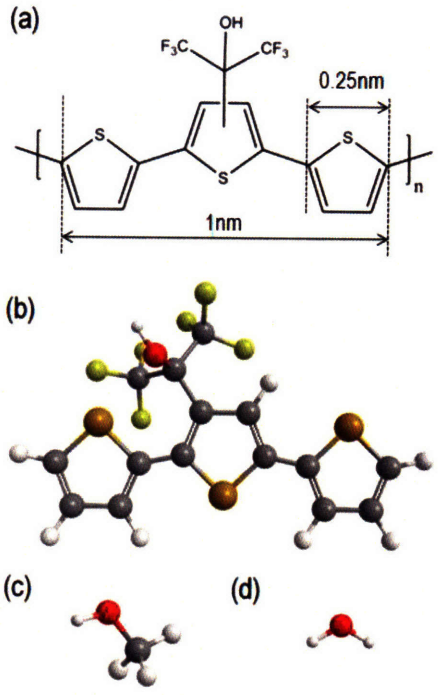

Figure 3-1. (a) Molecular structure of regiorandom HFIP-PT. The pendant group repeats every three units along the chain. The average number of repeat units per

chain corresponds to 24 and 44 for the 10kD and 18kD molecular weight samples both with a polydispersity index of 2.4. (b) Ball and stick model of the HFIP-PT monomer repeat, (c) methanol and (d) water molecules. The trithiophene unit is depicted in its planar configuration with all dihedral angles between thiophene rings set to 180°.

HFIP-PT was synthesized via oxidative polymerization from the terthiophene monomer (see Figure 3-2). The analysis of the NMR data reported earlier[71] (1H NMR (300MHz, CDCl3) δ: 7.26(aromatic C-H), 7.19 (aromatic C-H), 7.15(aromatic C-H), 3.97(O-H)) indicates that HFIP-PT is regiorandom. Hence, the average repeating unit of HFIP-PT presents 50% of the HFIP group in each possible position introducing an effective mirror plane normal to the chain axis at the center of the terthiophene, as illustrated in Figure 3-3.

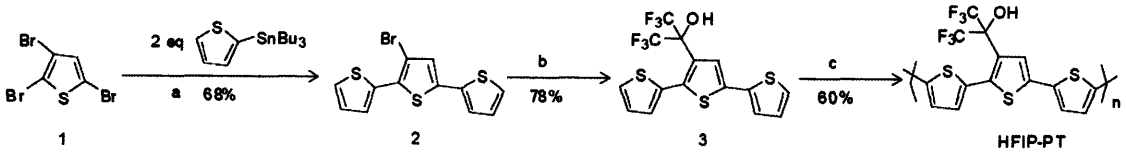

Figure 3-2. Synthesis of HFIP-PT. a: Pd(PPh3)4, DMF, 80°C; b: 1) n-BuLi, Hex/THF, -40°C; 2) Hexafluoroacetone, 0°C; c: Br2, HOAc, 60°C. Reproduced from Ref. [71].

Two batches of HFIP-PT were used in this study, one with an Mn of 10kD and another with an Mn of 18kD, both with a polydispersity index of 2.4. The average number of repeat units per chain corresponds to 24 and 44 for the 2 molecular weight samples. The 10kD HFIP-PT was used in the study of the gelation mechanism and the 18kD batch was mostly used to prepare thin films.

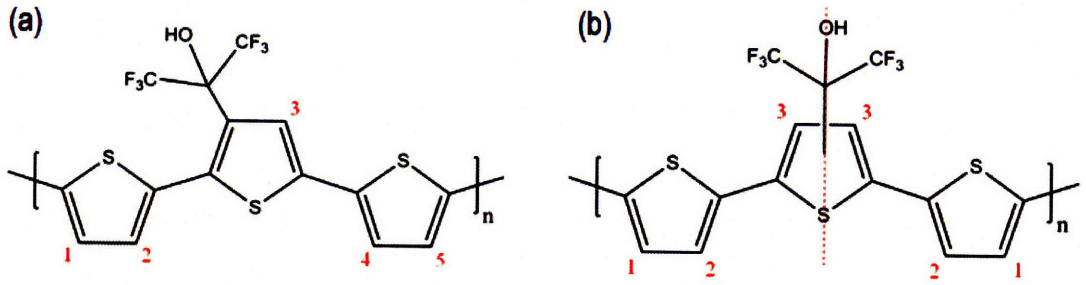

Figure 3-3. Distinctive aromatic C-H ^{1}H NMR signals in (a) regioregular and (b) regiorandom.

HFIP-PT shows good solubility in tetrahydrofuran (THF) and dimethyl methylphosphonate. It is less soluble in methanol, ethanol and isopropanol and it is insoluble in hexane, acetonitrile, ethylene glycol, glycerol and water.

3.1.2 Gelation Protocol

After precipitation and washing, the HFIP-PT formed a dried orange-red solid.[72] It was then readily dissolved in THF (Mallinckrodt Chemicals) at room temperature in a small glass vial. The concentration of the polymer in the initial THF solution was 0.32wt% for the particular preparation used for NMR and FTIR analysis.

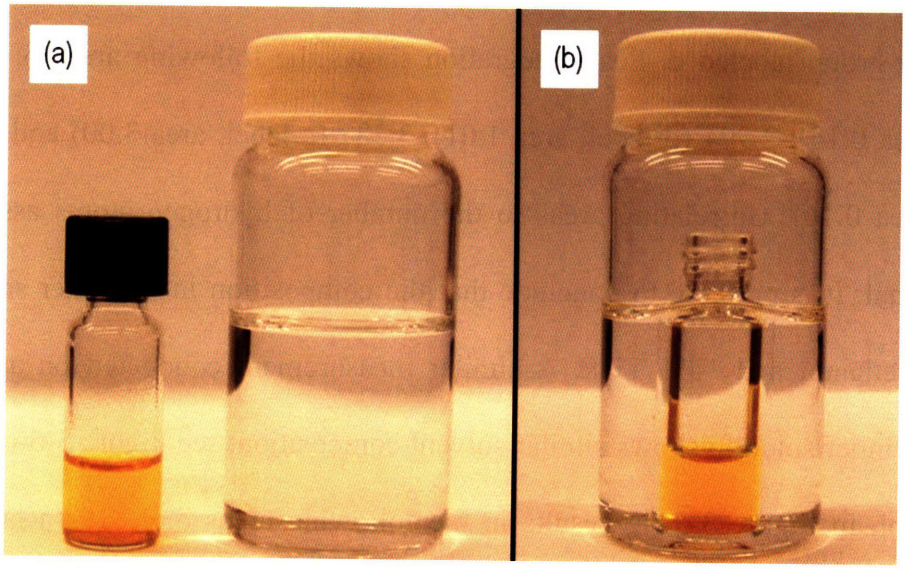

Figure 3-4. Procedure to induce exchange between THF and methanol in the polymer solution. (a) The small vial contains HFIP-PT dissolved in THF. The large vial contains methanol. (b) The small vial is contained in the larger one and diffusion between miscible solvents occurs up to equilibrium.

The small vial was placed in a larger glass vial containing methanol (Mallinckrodt Chemicals), see Figure 3-4. After 48h of solvent interdiffusion, the liquid in the small vial became turbid. NMR analysis is reported in Figure 3-5; both the liquid inside and outside the small vial had a composition of 96% methanol and 4% THF after 48h of solvents interdiffusion. The concentration of the polymer was too small to be detected by NMR analysis but is calculated to be 0.5wt%. In Figure 3-5-(a), the set of peaks centered at 1.815ppm and 3.701ppm are assigned to THF; a and b labeled hydrogens respectively. The peak at 3.387ppm is assigned to the hydrogens in methanol labeled c, and the peak at 2.994ppm to the hydrogen of the hydroxyl group labeled d. Peak integration shows the following areas δ: 1.815 (a label, area 0.14), 2.994 (d label, area 1.01), 3.387 (c label, area 3.00) and 3.701 (b label, area 0.14). Correlating areas to the number of hydrogen atoms assigned to each signal, it is possible to conclude that the composition in the outer solution is ~96% methanol and ~4% THF. A similar measurement conducted on an aliquot from the inner solution shows similar solvent composition, see Figure 3-5-(b). Peaks integration in Figure 3-5-(b) results in the following areas δ: 1.819 (a label, area 0.15), 2.994 (d label, area 0.99), 3.379 (c label, area 3.00) and 3.706 (b label, area 0.14). This measurement indicates that methanol diffused into the small vial and replaced THF as the major component of the initial HFIP-PT/THF solution.

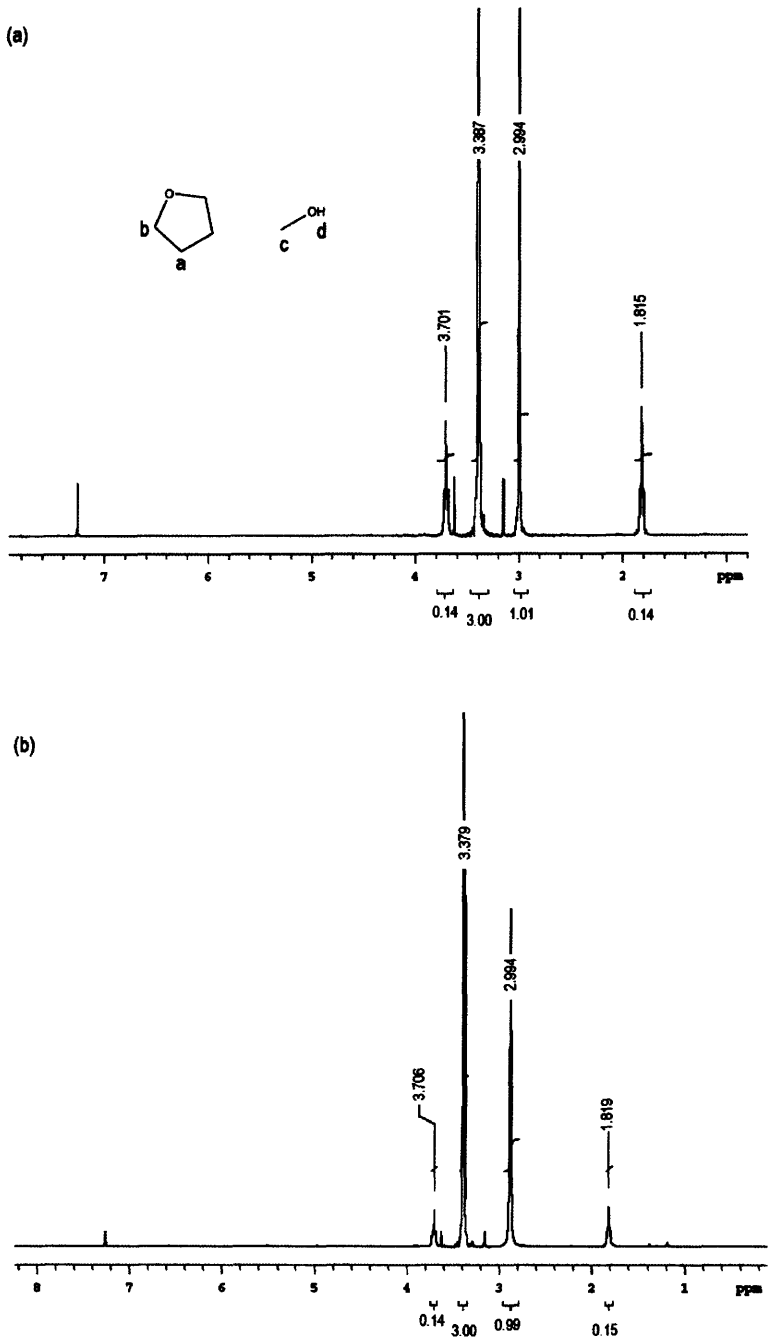

Figure 3-5. (a) ^{1}H NMR (300MHz, CDCl3) corresponding to the solution outside the small vial after 48h of solvents interdiffusion. (b) ^{1}H NMR (300MHz, CDCl3) corresponding to the solution inside the small vial after 48h of solvents interdiffusion.

Next, the liquid containing the polymer was transferred into a PTFE crucible and placed inside a fume-hood at room temperature and atmospheric pressure. Solvent evaporation in air resulted in the formation of an orange jelly-like substance. Under these conditions, water present in the ambient incorporated into the system. Thus, the gel contains HFIP-PT, methanol and water.

When desired, the gel in a bulk or thin film form was placed inside a desiccator containing anhydrous calcium sulfate (Drierite), connected to the vacuum line of a fume-hood with a pressure of 6Pa (0.045Torr).

3.1.3 Spectroscopy and Microscopy Techniques

NMR spectroscopy was conducted using a Varian Mercury (1H NMR, 300MHz, CDCl3). FTIR spectroscopy was performed on a Perkin-Elmer 2000 using KBr window cards as support (Sigma Aldrich, Real Crystal™ IR). NMR and FTIR studies were conducted in Department of Chemistry Instrumentation Facility at MIT. Light microscopy (LM) analysis was done employing a Zeiss Axioskop and a Zeiss Axioskop 2 at the MIT's Institute for Soldier Nanotechnologies.

3.2 Gelation Mechanism

THF is a good solvent for HFIP-PT, methanol is a poor solvent, and water is a non-solvent. After 48 hours of methanol interdiffusion into the THF-polymer solution, the solution becomes turbid. The increasing concentration of methanol induces the chains to cluster, most likely due to the combined enthalpic effect of the strong CH_3OH-HFIP associations and polymer-polymer chain interactions. The sample is then transferred into a crucible where solvent evaporation at ambient pressure inside a fume-hood results in the formation of an orange jelly-like substance (estimated polymer concentration is 2 wt %). The gel contains HFIP-PT, methanol and water which is incorporated from the ambient moisture.

Figure 3-6 shows a polarized light microscopy image of the gel taken from the crucible. The depolarization of incident light suggests an isotropic distribution of locally anisotropic clusters in the bulk gel. In contrast, the strong birefringence present in the lower-right corner in Figure 3-6 reveals the ability of the material to easily deform into a globally anisotropic morphology (likely due to handling the gel).

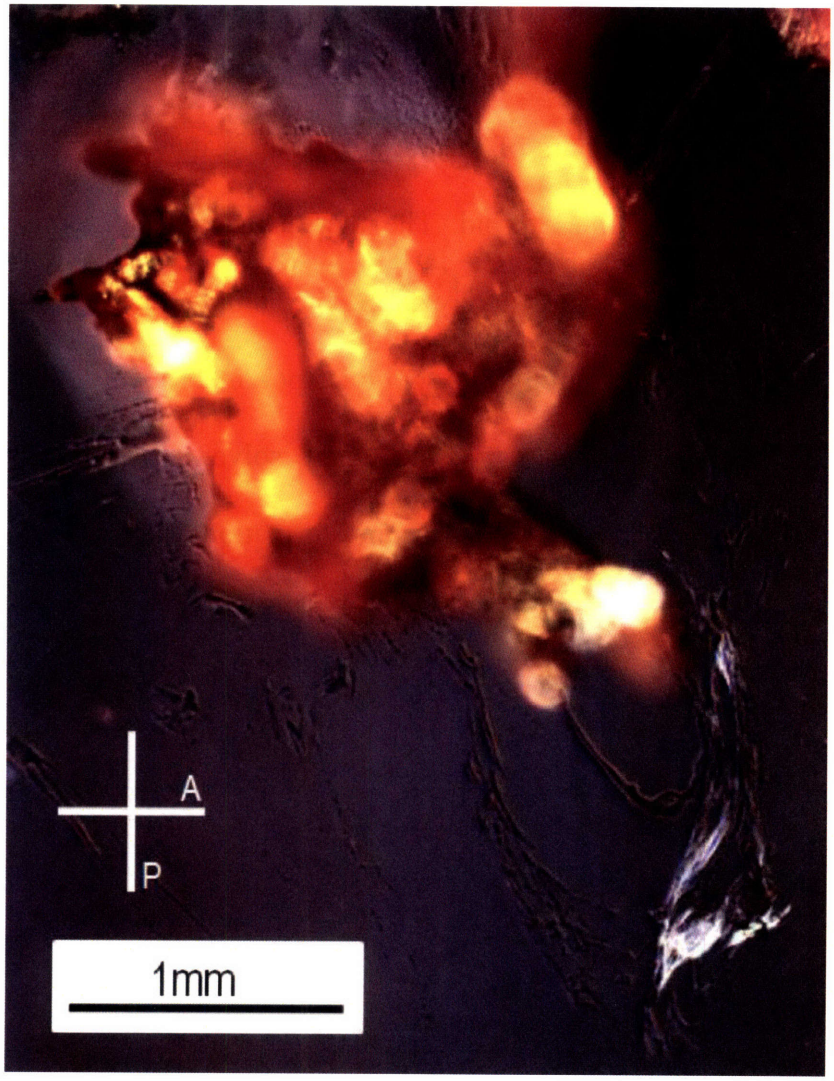

Figure 3-6. Polarized light micrograph of a piece of HFIP-PT gel deposited on a glass slide. The gel readily turns into a globally anisotropic morphology upon accidental deformation with the spatula as illustrated by the thin birefringent region at the lower-right corner.

In order to investigate the governing interactions behind gel formation we used FTIR spectroscopy to follow the initial build up in methanol concentration and then the vacuum assisted decrease in solvent concentration. After 0.5h, 1.5h, 4h, 24h and 48h exposure to methanol vapors, a drop from the initial polymer THF solution is cast onto a KBr window card. FTIR analyses of the initial HFIP-PT solution in THF (0h) and of the gel are also conducted. Further FTIR measurements are conducted to evaluate the decrease in solvent concentration upon residence under vacuum. For this, each preparation on a KBr window card is interrogated by FTIR after 2h, 24h and 48h under a vacuum of 6Pa (0.045Torr). The concentration of solvent in the gel decreases under these conditions, representative FTIR series as a function of decreased solvent content are reported in Figure 3-7. Samples are labeled as follows: exposure time to methanol vapors/time under vacuum, e.g. 48h/48h indicates the initial HFIP-PT solution in THF was exposed to methanol vapors during 48h before being cast onto a KBr window card which was further placed under vacuum for 48h.

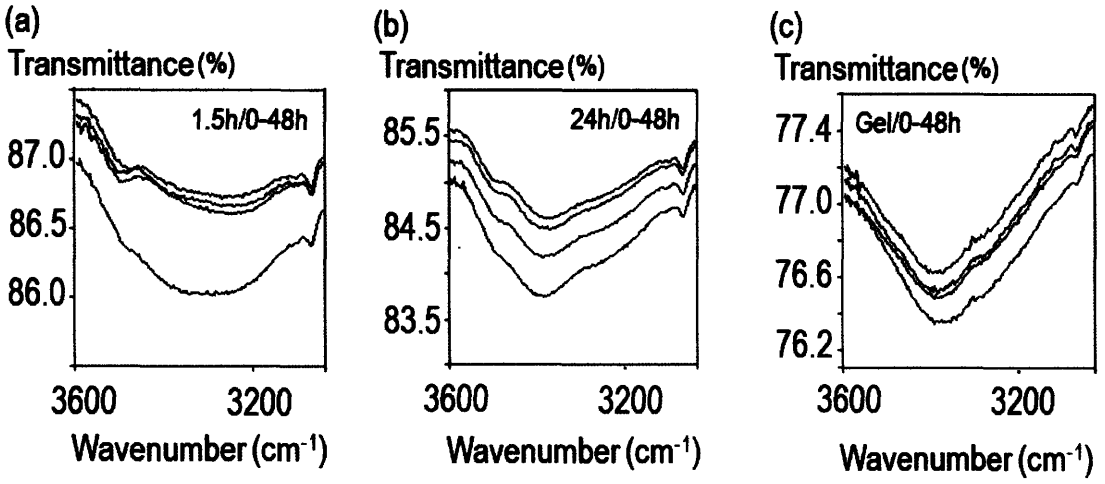

Figure 3-7. FTIR spectra of representative drying series. (a) 1.5h/0h, 1.5h/2h, 1.5h/24h and 1.5h/48h (b) 24h/0-48h (c) Gel/0-48h. For each interdiffusion time, higher transmittance spectra correspond to longer times under vacuum.

Figure 3-8 shows a set of FTIR spectra for the following samples 0h/48h, 0.5h/48h, 1.5h/48h, 4h/48, 24h/48h, 48h/48h and Gel/48h. The left window spans a frequency range relevant to O-H stretching mode and the right window to C-O stretching mode, see Table 3-1. [73] After 24h interdiffusion, a broad peak emerges in the region 3600-3200cm^{-1} (labeled a) in the left window in Figure 3-8. It remains at longer interdiffusion times and it is also evident in the gel spectrum. Its center varies between 3380 and 3366cm^{-1}. The peak is located at a frequency close to the broad band found in the molten phase spectrum of tert-butyl alcohol (3362cm^{-1}).[74] Liquid methanol exhibits a broad band centered at 3342cm^{-1}. The emergence of a broad band in the 3600-3200cm^{-1} spectral region during interdiffusion of CH_3OH and THF

is indicative of an increased degree of hydrogen bonding network. The center of the emerging band a is located at lower frequencies compared to the narrower peaks at 3640cm^{-1} and 3500cm^{-1} (labeled b and c respectively). The two narrower b and c peaks could be assigned to O-H stretching in the non-H-bonding regime, see Table 3-1. This interpretation seems to be further supported with the top spectrum where both the b and c peaks vanish. The absence of peaks assigned to non-H-bonded O-H stretching in the gel, jointly with the emergence of the hydrogen bonding band, is indicative of a high degree of hydrogen-bonding between solvent molecules and HFIP groups.

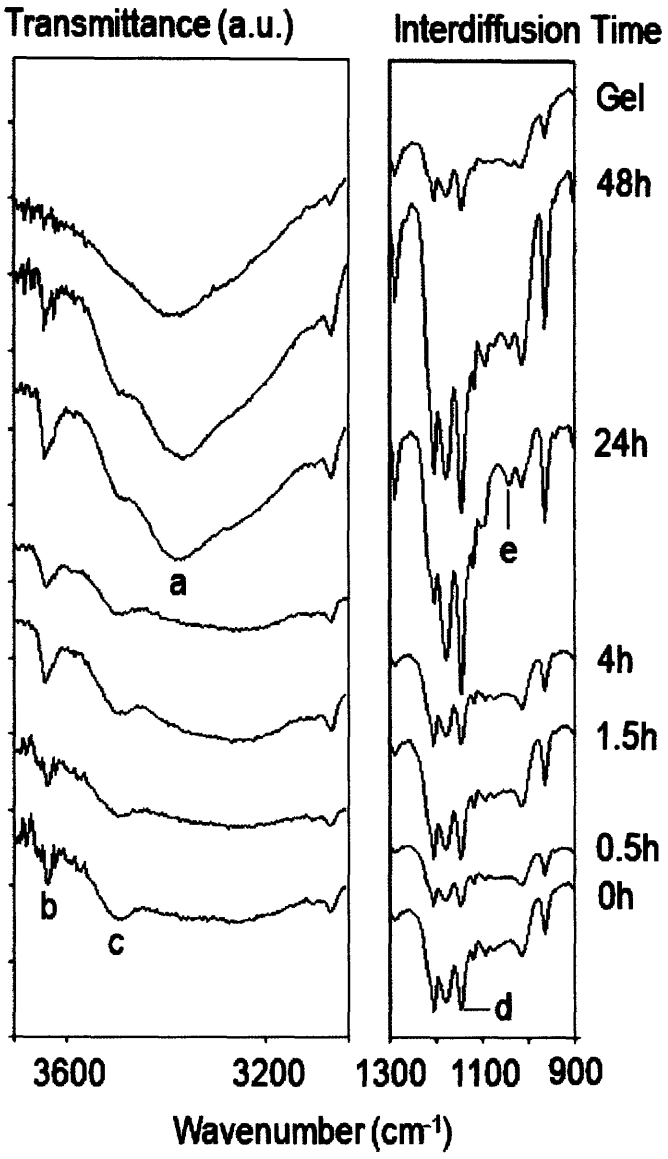

Figure 3-8. FTIR spectra as a function of solvent interdiffusion time. Spectra were taken after each sample has held for 48h under house vacuum of 6Pa (0.045Torr). Specific regions of interest are labeled a-e: a: 3375cm^{-1}, b: 3640cm^{-1}, c: 3500cm^{-1}, d: 1150cm^{-1}, e: 1055cm^{-1}.

In the frequency range corresponding to the C-O stretching mode, right window in Figure 3-8, primary alcohols appear at ~1050cm^{-1} and tertiary alcohols are located at ~1150cm^{-1}. The peak appearing at ~1150cm^{-1} in all spectra (labeled d) could be assigned to C-O stretching of the hydroxyl group in HFIP. Only in the spectra corresponding to longer interdiffusion times (24h and 48h) and to the gel, does a signal emerge at 1055cm^{-1}, labeled e, which is assigned to the C-O stretching band of methanol.

Table 3-1. Selected group frequencies for O-H and C-O vibrational modes. [a]

Group frequency wavenumber (cm^{-1})	Assignment
3570-3200 (broad)	O-H stretch (H-bonded hydroxy group)
3645-3600 (narrow)	O-H stretch (Nonbonded hydroxy group)
3645-3630	O-H stretch (Primary alcohol)
3620-3540	O-H stretch (Tertiary alcohol)
~1050	C-O stretch (primary alcohol)
~1150	C-O stretch (tertiary alcohol)

[a] Reproduced from reference [74].

3.3 Chapter Conclusions

The incorporation of HFIP to PT allows the polymer to form a gel. The interpretation of FTIR measurements indicates that at least one of the molecular interactions responsible for gelation is based on hydrogen bonding associations and that methanol is retained in the gel even after being under vacuum of 6Pa for 48h. Figure 3-9 is a schematic of the H-bonding linkage between HFIP-PT and methanol at the crosslinking site.

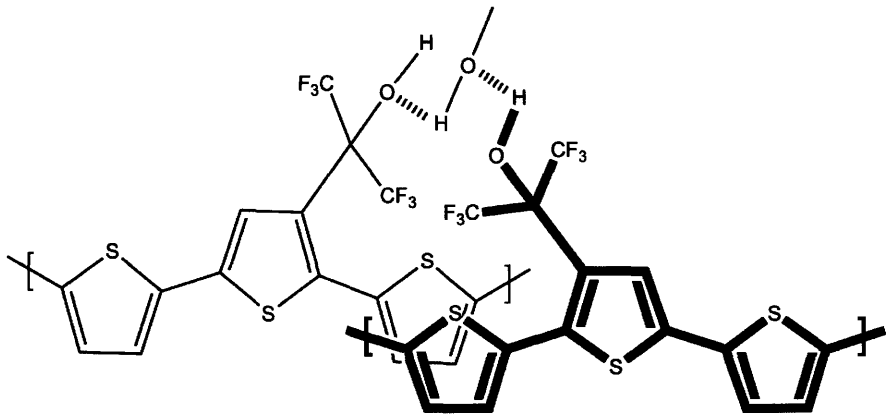

Figure 3-9. Schematic of HFIP-PT and methanol chemical structures illustrating the H-bonding association at the crosslinking site.

Chapter 4

Oriented Gel Films

We were motivated to find a processing pathway to form a highly oriented HFIP-PT morphology for future structure-property studies. A detailed investigation of the structure at the molecular level is sought in view of applications where a controlled orientation of the chains is relevant. Moreover, having a highly swollen but highly oriented PT gel is a useful starting material for doping to create electrically conductive films and for analyte sensing films due to facile diffusion of new components into the film. Section 4.1 dedicates to the experimental part; film processing and characterization techniques. In Section 4.2, we describe the morphology and structure of HFIP-PT gels based primarily on transmission electron microscopy (TEM) and XRD techniques.

4.1 Procedure

4.1.1 Film Processing

The entire process to prepare films is summarized in Figure 4-1. The detailed procedure follows:

(1) The gel was first deposited on a glass slide on a Koefler bench (Leica Aktiengesellschaft) and heated to 100°C in about 15s. At this temperature, the gel melted. During heating, it is possible that water from the ambient moisture could further replace methanol in the gel as it is able to form stronger hydrogen bonding associations.

(2) The molten gel/glass slide was removed from the heating stage and transferred to a substrate at room temperature.

(3) After 15s, the razor blade was used to shear the melted gel during cool-down; one pass per film at an angle of ~30°.

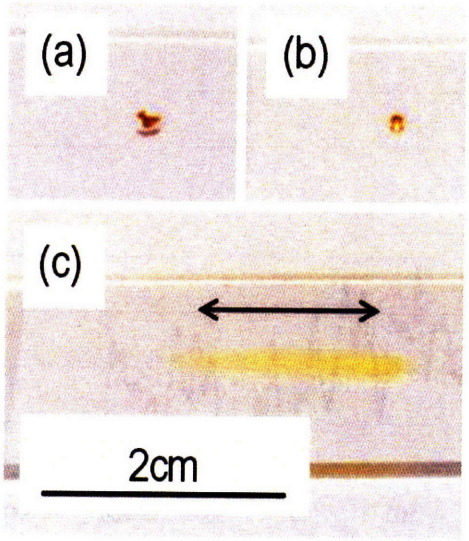

Figure 4-1. Preparation of oriented gel films. (a) Piece of gel on a glass slide. (b) A drop of molten gel after being heated at 100°C. (c) A razor blade is used to shear the gel.

After shearing, films had a rectangular shape with area about $10x2mm^2$. The procedure employed resulted in tapering film thicknesses. The average thickness on the thinner region is 1.8μm (σ = 0.5μm) and on the thicker region is 5.4μm (σ = 1.4μm). Figure 4-2 illustrates two representative scans of thin films profile.

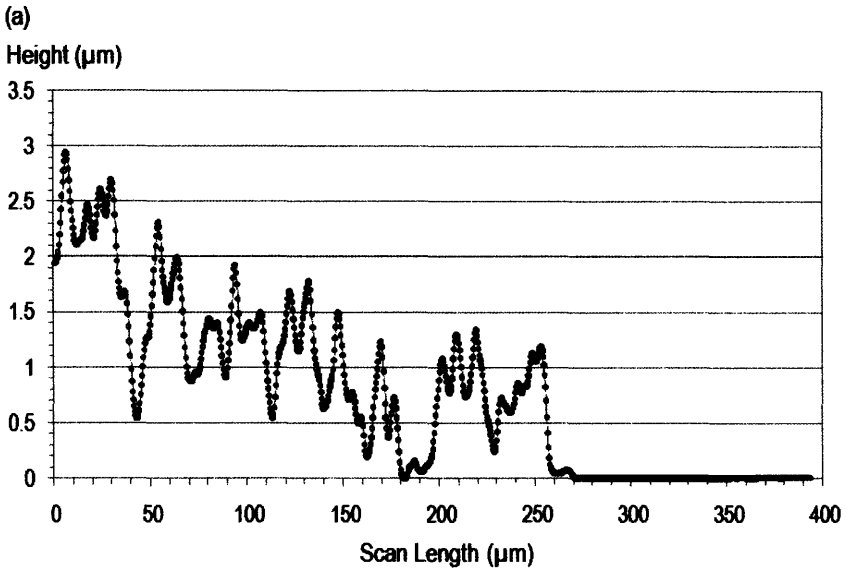

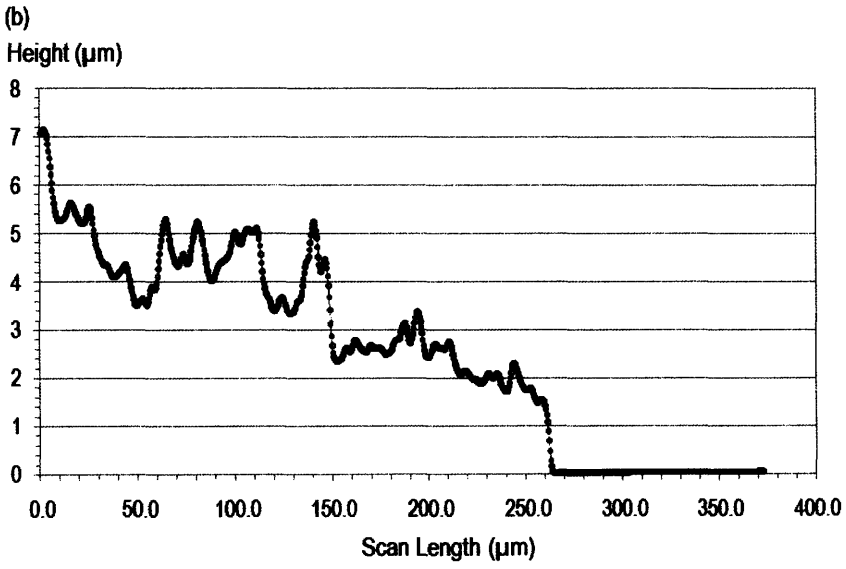

Figure 4-2. Typical surface profiles for the (a) thin and (b) thick regions of a tapered gel oriented film. They correspond to the end and starting regions as the film is sheared respectively. The line scans correspond to the edge of the film, the flat region on the right side is the glass substrate.

4.1.2 Characterization Techniques

LM analysis was done employing a Zeiss Axioskop and a Zeiss Axioskop 2. Film thickness was evaluated on a Tencor P-10 Surface Profilometer. Thermal stability and optical anisotropy of oriented thin films were evaluated with regard to variations of the intensity of reflected polarized light on a LM with an Oriel spectrometer attached. The optics used in the optical anisotropy analysis of oriented gel films are based on the standard setting used in differential interference contrast but working in reflectance mode. In this set-up, a Wollaston prism above the objective lens separates the light polarized by the first filter into two rays polarized at 90°. Light polarized at 45° arrives at the polymer film, some rays are transmitted and get reflected on a mirror. Light comes back to the film and ends up at the spectrophotometer. Chains act as a grating, the maximum intensity of reflected polarized light corresponds to the chains being aligned parallel to the polarizing filter (45°) and the minimum when oriented at plus or minus 45° with respect to the filter (0° and 90°). Changes in the intensity of reflected light were correlated to the degree of in plane optical anisotropy by rotating the film on the LM stage. Thermal treatment was conducted on a Linkam THMS600 stage with TP94 single ramp temperature controller coupled to the LM.

TEM was performed on a JEOL 2000FX and on a JEOL 2011. Both instruments were operated at 200kV. The vacuum in the TEM specimen chamber

was ~10^{-5}Pa. Bright-field images and diffraction patterns were recorded with an AMT camera system. Due to the beam sensitivity of the sample, TEM was performed under low dose conditions so as to have a sufficient lifetime to record diffraction patterns. Diffraction pattern calibration was done with an evaporated aluminum standard (Electron Microscopy Sciences) at the same acceleration voltage and objective lens setting. Oriented gel films suitable for TEM analysis were coated with a 25nm carbon film on a Denton Vacuum DV-502A evaporator with a nominal vacuum of ~10^{-4}Pa. Selected regions of carbon-coated films were detached from the glass support using polyacrylic acid backing (Alfa Aesar) and transferred to a standard 200 mesh TEM grid (Electron Microscopy Sciences, G200-Cu).

XRD analysis of thin films (2x10mm2 and 3μm thick) oriented on glass substrates was performed on a Rigaku RTP500RC instrument operated in Bragg-Brentano geometry with Cu Kα radiation (λ=0.154nm). Figure 4-3 illustrates the geometries for both electron and x-ray diffraction techniques.

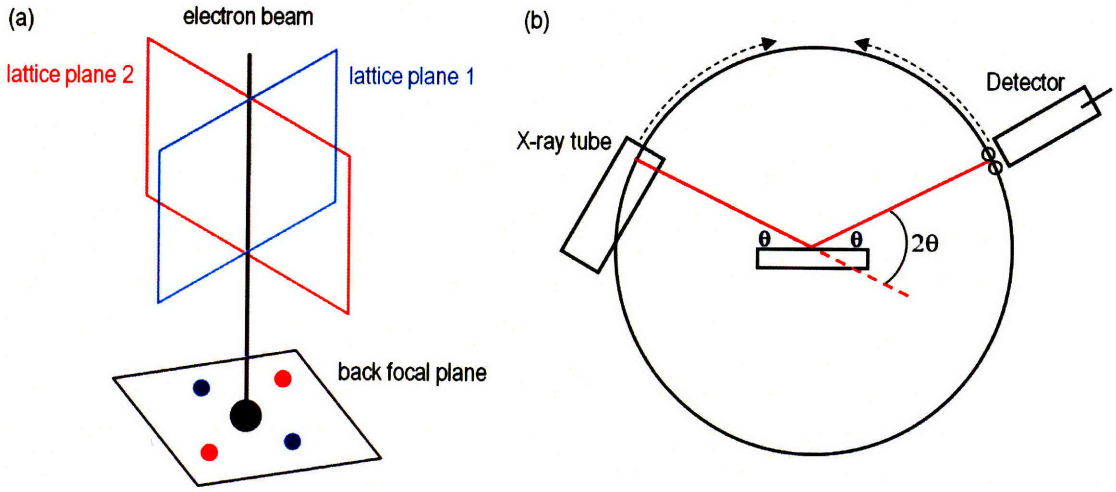

Figure 4-3. (a) Schematic of diffraction in parallel beam TEM, the zone axis is parallel to the electron beam. (b) Bragg-Brentano geometry used in XRD analysis. This particular motion corresponds to a θ:θ instrument. Reproduced from reference [Figure 4-3-(a) follows Professor Gradecak's lecture notes, 3.34 Imaging of Materials, Department of Materials Science and Engineering, MIT Spring Term 2008. Figure 4-3-(b) is reproduced from Dr. Speakman's seminar, Basics of X-Ray Diffraction. MIT's Independent Activities Period, January 2008].

4.2 Structure and Stability of Oriented Films

4.2.1 Light Microscopy

Thin films were prepared by hand shearing using a razor blade on a glass slide. The Gel/0h was first heated at 100°C, it melted and then shearing was conducted during cooling and an oriented gel reformed. Oriented gel films present

an essentially uniform birefringence as illustrated in Figure 4-4-(a). The changes in intensity are attributed to local variations in film thickness jointly with the presence of unoriented pieces of gel. When the melted gel is sheared immediately after heating, i.e. at a temperature close to 100°C, the resulting film is not birefringent. This suggests that stress transfer and retention necessary to induce alignment between chains during deformation requires the network of hydrogen bonding crosslinks and chain-chain interactions to build up in the system, the gel reforms at lower temperatures.

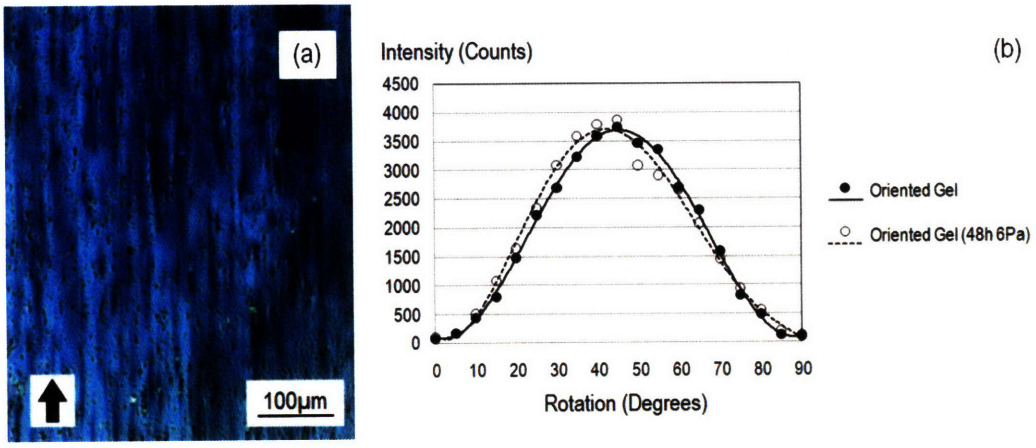

Figure 4-4. (a) Cross-polarized light micrograph of an HFIP-PT oriented gel film. The film was prepared by blade shearing the melted gel during cool-down. The shearing direction is illustrated by the arrow. The small dark entities observed are unoriented gel fragments. (b) Optical anisotropy analysis of oriented gel films. The number of counts corresponds to the intensity of the reflected polarized light at 540nm.

When the Gel/0h is placed under vacuum, the solvent concentration decreases as indicated by FTIR analysis, see Figure 3-7-(c). Nevertheless, the gel retains enough methanol and water to be melted and then deformed into oriented anisotropic films. Solvent concentration in the gel after 48h at 6Pa is estimated at 12wt%.[75] This suggests an ideal gel composition consisting of a minimum content of gelling molecules at which plasticity can still be possible with minimal interference in chain packing during mechanical deformation at an optimal temperature.

The degree of in-plane optical anisotropy is illustrated in Figure 4-4-(b). Analysis is conducted on 2 oriented films, both films prepared by shearing the molten gel (Gel/0h) during cooling from 100°C. One film, corresponding to the dashed line in Figure 4-4-(b), was further placed under vacuum of 6Pa during 48h prior to analysis. The full width at half maximum (FWHM) of the intensity of the reflected polarized light as a function of rotation angle for both preparations is ±23° for a sampled area of $3mm^2$. The simple procedure followed to prepare the films and the presence of solvent may contribute to this misalignment.

The thermal stability of oriented films is evaluated by monitoring the variation in intensity of reflected polarized light with temperature. Sample preparation for this analysis consists on shearing the molten gel (Gel/0h) during cool-down from 100°C and then placing the oriented film under vacuum of 6Pa during 48h. The results are reported in Figure 4-5. Upon heating, the degree of

orientation in the film drops continuously in the 55 to 70°C range. No recovery of global orientation is observed upon cooling. After loss of orientation, the film can be recovered from the glass slide, reheated and reoriented into an anisotropic morphology.

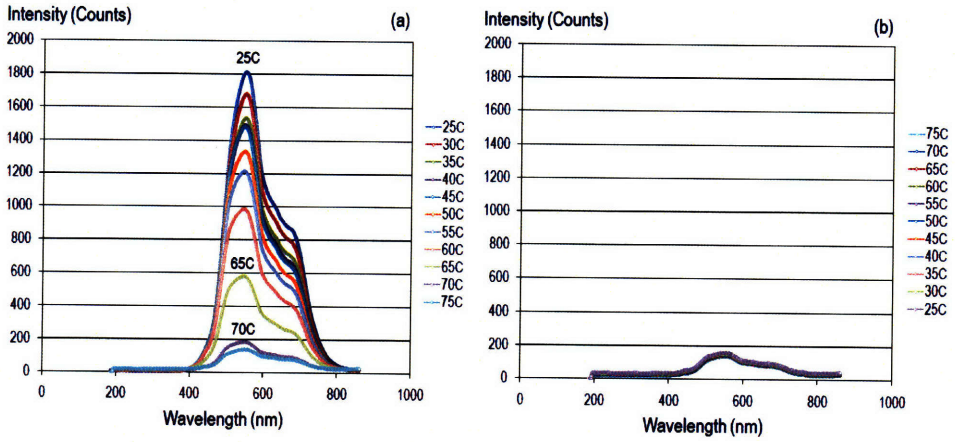

Figure 4-5. Reflectivity spectra monitoring the change in intensity of reflected polarized light with temperature of an oriented gel film that has been further placed under vacuum (48h 6Pa). (a) Heating ramp. (b) Cooling ramp. Thermal treatment consisted of heating at a rate of +1°C/min from 25°C to 75°C and cooling at a rate of -1°C/min from 75°C to 25°C. The residence time at 75°C was negligible.

4.2.2 X-Ray Diffraction

XRD characterization of oriented gel (Gel/0h) films (2x10mm^2 and 3μm thick) shows a peak maximum corresponding to an interplanar spacing of 0.42nm

normal to the plane of the film and 2 additional peaks at higher angles as illustrated in Figure 4-6. These 3 peaks would correspond to (h_1k_10), (h_2k_20) and (h_3k_30) respectively. The FWHM for the (h_1k_10) peak is 1° (instrumental FWHM at this angle is 0.1). Two factors that could contribute to the peak broadening are a distribution of d spacings normal to the chain axis and size broadening due to crystalline clusters of sizes below about 10nm.

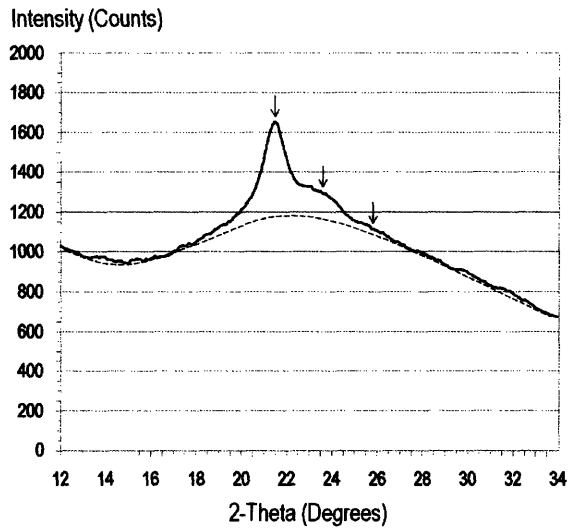

Figure 4-6. XRD analysis of an HFIP-PT oriented gel film. 3 peaks are observable, the peak at lower angles would corresponds to $d(h_1k_10)$=0.42nm spacing normal to the plane of the film and the 2 additional peaks at higher angles to $(h_2\ k_2\ 0)$ and $(h_3\ k_3\ 0)$ respectively.

4.2.3 Electron Imaging and Diffraction

TEM analysis was done on the thinnest regions at the tapering edge of a shear oriented gel (Gel/0h). These regions have likely undergone the greatest deformation. Films suitable for TEM analysis were coated with a 25nm carbon film. Selected regions of carbon-coated films were detached from the glass support using polyacrylic acid backing and transferred to a standard TEM grid. The electron diffraction pattern in Figure 4-7-(a) corresponds to the normal projection along the chain axis. This analysis indicates that the HFIP-PT chains lie in the plane of the film and that they are highly aligned parallel to the deformation direction. The direction along the chain axis is assigned to the crystallographic c axis. The strong equatorial reflections are indicative of a parallel stacking of HFIP-PT chains in the plane of the film. The direction normal to the chain axis and in the plane of the film is assigned to $[h_1k_10]$ with $d(h_1k_10) = 0.42$nm. An additional weak and diffuse equatorial reflection is observable. The spacing is around 0.21-0.24nm which could correspond to the second order of the strong inner reflection with spacing 0.42nm.

In P3HT an interchain π–π stacking distance of 0.38nm is assigned between successive polythiophene backbones.[76] The fiber pattern in Figure 4-7-(a) also presents strong equatorial reflections which could correspond to the parallel stacking distance between HFIP-PT conjugated backbones. The higher spacing of 0.42nm found in HFIP-PT oriented gels compared to P3HT could be the consequence of a

less dense chain packing due to the absence of regioregularity, to the size of the HFIP pendant group and to the presence of solvent.

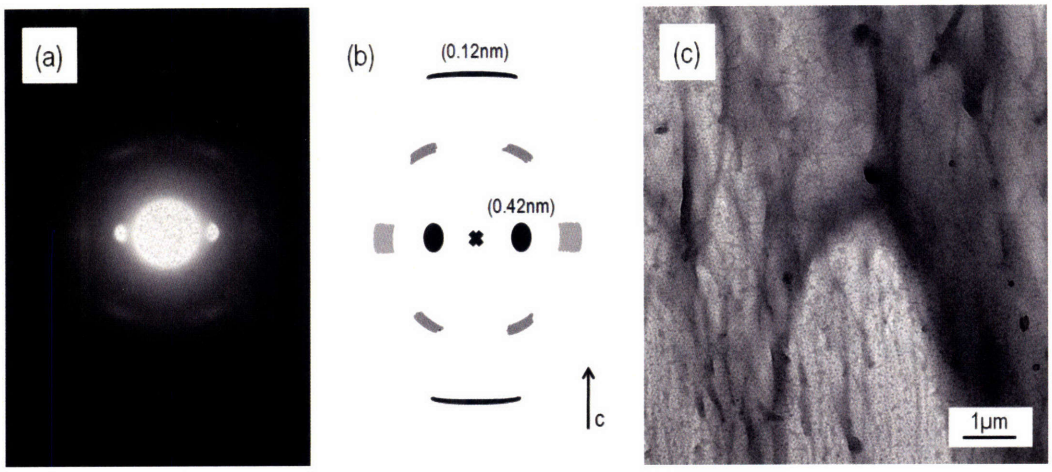

Figure 4-7. (a) Electron diffraction pattern of an oriented HFIP-PT film. Contrast has been digitally enhanced. (b) Schematic of the sheared film diffraction pattern. Labeled reflections have distances corresponding to spacings in direct space. The strong equatorial and meridional reflections are representative of a parallel stacking of uniaxially aligned chains in the plane of the film. (c) Bright-field TEM micrograph corresponding to the area contributing to the diffraction pattern. An overall aligned texture is evident with mass thickness contrast arising from thickness variations of the film.

The arced meridional reflections in Figure 4-7-(a) correspond to a period of 0.12nm along the c axis. This distance is approximately half the width of one thiophene ring (see Figure 3-1). This periodicity along the chain axis suggests that

the conjugated backbones are shifted with respect to each other neighbors by half the thiophene length, yielding an interdigitation of the pendant groups. The regiorandom nature of HFIP-PT and the steric interactions between HFIP groups could contribute to the axial shift between neighboring chains. The meridional reflections give an azimuthal arcing of approximately ±10° which corresponds to less than half the magnitude obtained from the optical anisotropy analysis in the LM. This is likely due to the increased amount of shearing in the thinnest regions of the film and the smaller sampled area (Selected area for diffraction in the TEM was ~100μm^2 while in the optical anisotropy analysis in the LM was ~3mm^2). Additional diffuse reflections are observable with spacing around 0.20-0.23nm. The presence of these (hkl) reflections suggests a three-dimensional order in oriented gel films.

The rigid nature of the HFIP-PT chains, polymer-polymer interactions and the proximity of the hydroxyl group in HFIP to the PT backbone allow chains to align upon mechanical orientation. The lack of regioregularity, however, is a limiting factor to achieve a full crystallographic registry between stacked chains and possibly to attain an overall crystalline configuration except in the most densely packed regions. Figure 4-8 is a model of the morphology of oriented gel films and of the local arrangement of chains and solvent molecules in the highly crystalline clusters. In Figure 4-8-(a) only the distribution of HFIP-PT chains is depicted, we suggest the existence of tie points in the form of paracrystalline clusters in an overall swollen network. Figure 4-8-(b) summarizes the molecular level analysis of the highly

oriented regions: (1) HFIP-PT chains lie in the plane of the film, (2) there is a parallel π-π stacking of uniaxially aligned backbones and (3) a network of linkages based on chain-chain interactions and hydrogen bonding associations between HFIP groups and small polar protic molecules is necessary for stress transmission and retention upon mechanical orientation during gel reformation from the molten state.

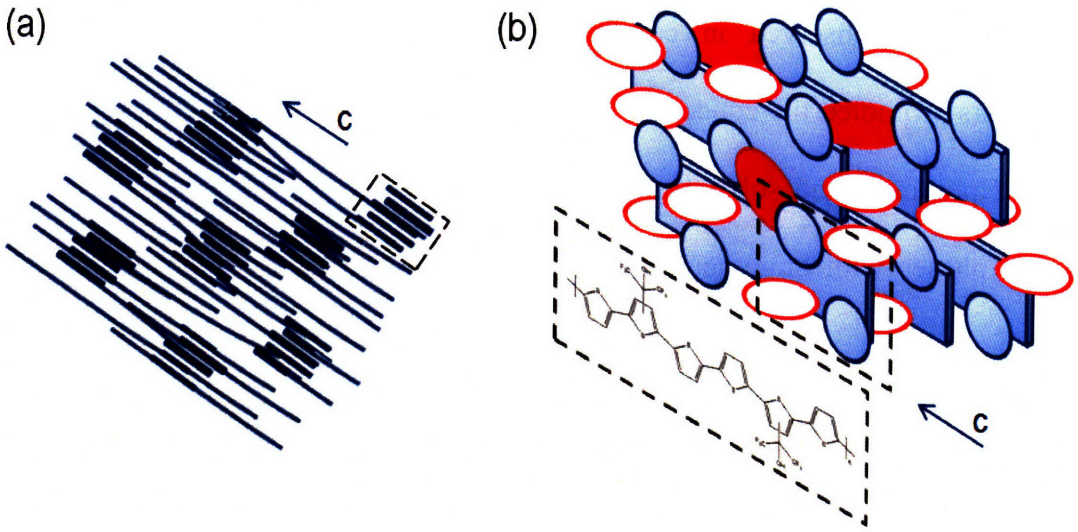

Figure 4-8. (a) Model of the morphology of HFIP-PT oriented gel films suggesting an anisotropic distribution of paracrystalline regions in an overall swollen network (Only polymer chains are depicted). Thicker segments are included to help visualize a more dense packing between chains in the crystalline clusters. While chains in between ordered phases are depicted in a rigid-like configuration, the high solvent concentration is expected to limit their crystallinity. (b) Molecular packing in the crystalline clusters. The blue strips represent the PT backbones and the attached blue ovals the HFIP pendant groups. The elongated darker ovals (red) connecting

pendant groups represent the reversible crosslinks based on hydrogen bonding associations between HFIP pendant groups and polar protic molecules (methanol and water). The proximity between conjugated backbones is representative of the effect of direct polymer-polymer associations on the internal packing in ordered clusters. The white elongated ovals represent solvent molecules interleaving between chains.

The highly crystalline regions in HFIP-PT gels appear similar to the crystal-solvate phases observed in certain solutions of rigid polymers. Papkov and coworkers promoted the concept of crystal-solvate to describe the co-crystallization of rigid polymers and solvent molecules.[77] Rigid polymers can also form crystal-solvate phases with oligomeric solvents, such as the case of of poly(p-phenylene benzobisthiazole) solutions in poly(phosphoric acid). In this system, Thomas and Cohen observed a phase transition to the solid state driven by the action of water as coagulant during film and fiber spinning from a poly(phosphoric acid) solution in the nematic state resulting in highly oriented parallel packing of polymer and oligomer phosphoric acid chains.[78]

4.3 Chapter Conclusions

Hexafluoroisopropanol functionalized polythiophene is able to build up a self-supporting network structure based on a combination of polymer-polymer chain interactions and the association of HFIP pendant groups with small polar protic molecules through hydrogen bondings. These thermally reversible physical crosslinks incorporate plasticity into the conjugated polymer gel. Under balanced combination of mechanical stress and temperature, the gel can be processed into thin films with the chains highly aligned along the shearing direction. We suggest the gel morphology comprises a distribution of crystalline clusters in an overall swollen network. In these ordered regions conjugated backbones are π-stacked with respect to each other neighbors and lie parallel to the substrate. The mechanically induced structural rearrangement from an isotropic to an anisotropic conjugated polymer gel occurs when transitioning from the molten state to the gel state.

Chapter 5

Oriented Gel Fibers

Fiber drawing is a processing technology that can yield a high degree of chain orientation. An exploratory study on gel drawn fibers was conducted in order to evaluate the potential of HFIP-PT gel plasticity under similar tensile conditions. In section 5.1, we describe the experimental details followed to prepare fibers and the techniques employed for their structural characterization. In section 5.2, we report the main results of the structural analysis of oriented gel fibers.

5.1 Procedure

The preparation of HFIP-PT fibers is described in Section 5.1.1. The experimental details of LM and TEM characterizations are reported in Section 5.1.2.

5.1.1 Fiber Processing

Fibers were simply prepared by pulling a piece of heated gel between the ends of a pair of tweezers. During cooling, a fragment of a pre-heated gel was clamped between the tips of a pair of tweezers. The tweezers were opened and a fiber pulled in between both ends as illustrated in Figure 5-1. The detailed procedure follows:

(1) A piece of gel was transferred from the crucible onto a glass slide, see Chapter 3 for experimental details concerning the preparation of HFIP-PT gels. The estimated polymer concentration in the gel is 2 wt %.

(2) The glass slide/gel was deposited on a Koefler bench (Leica Aktiengesellschaft) and heated to 100°C. At this temperature, the gel melted.

(3) The glass slide/molten gel was removed from the heating stage and deposited on a substrate at room temperature.

(4) A fragment of the molten gel was clamped between the tips of a pair of tweezers (Electron Microscopy Sciences, No. 78518-3C).

(5) The pair of tweezers opened and a fiber pulled in between both ends during cool-down. Drawn fibers were typically on the order of 15μm in diameter as illustrated in Figure 5-2.

(6) Finally, the fiber was deposited on a suitable substrate for LM or TEM analysis, e.g. a glass slide or a carbon coated mica substrate.

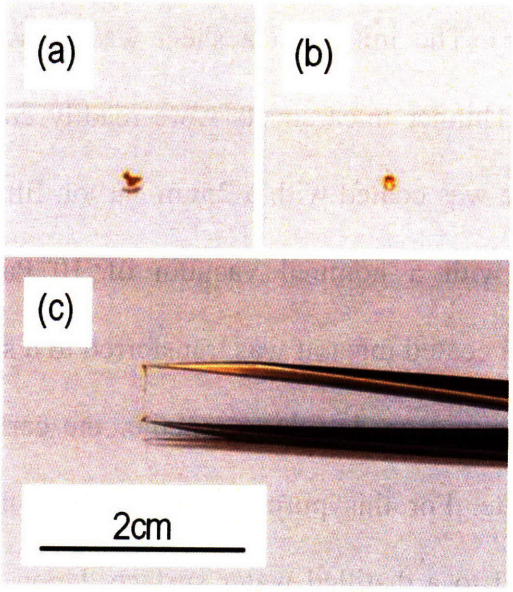

Figure 5-1. Procedure followed to draw fibers. (a) Piece of gel deposited on a glass slide. (b) Molten gel drop at a temperature close to 100°C. (c) Fibers pulled in between the ends of a pair of tweezers.

5.1.2 Light and Electron Microscopies

LM and TEM characterization of oriented fibers followed the procedures employed in Ch.4 for the analysis of oriented gel films except for TEM sample preparation.

After a fiber was drawn between the ends of a pair of tweezers, the fiber was deposited onto a 25nm thick carbon coated mica substrate. The carbon coated mica support was previously prepared from a 0.3mm thick and 25x75mm in size mica sheet (Electron Microscopy Sciences, muscovite mica, V-5, 25x75mm, thickness 0.26-0.31mm). The initial mica sheet was cleaved into thinner sheets, about 0.1mm or less. Thinner mica sheets were readily cut with scissors and the freshly exposed surface was coated with a 25nm carbon film on a Denton Vacuum DV-502A evaporator with a nominal vacuum of 10^{-4}Pa. Once the fiber was deposited on the carbon coated mica, it was transferred to a standard 200 mesh TEM grid. This transfer consisted on detaching together the carbon film with the fiber from the mica substrate. For this purpose, the edge of the carbon coated mica substrate was presented to a distilled water surface. Upon contact with water, the surface tension caused the carbon film to float off the mica sheet. The fiber lying on the carbon film remained on the water surface where it was recovered with a TEM copper grid.

Electron diffraction pattern calibration was done with an evaporated aluminum standard (Electron Microscopy Sciences) at the same acceleration voltage and objective lens setting employed during the study of fibers.

5.2 Structure of Drawn Fibers

The structural study of oriented gel fibers combines the analysis of light microscopy observations reported in Section 5.2.1 with imaging and diffraction measurements in the TEM, Section 5.2.2.

5.2.1 Light Microscopy

The arrows in Figure 5-2-(b) indicate the formation of necked regions upon fiber drawing. The applied stress field increases in the vicinity of a necked region which results in a higher degree of deformation. In fiber processing of crystallizable polymers, it is known that necking results in high degree of chain orientation.

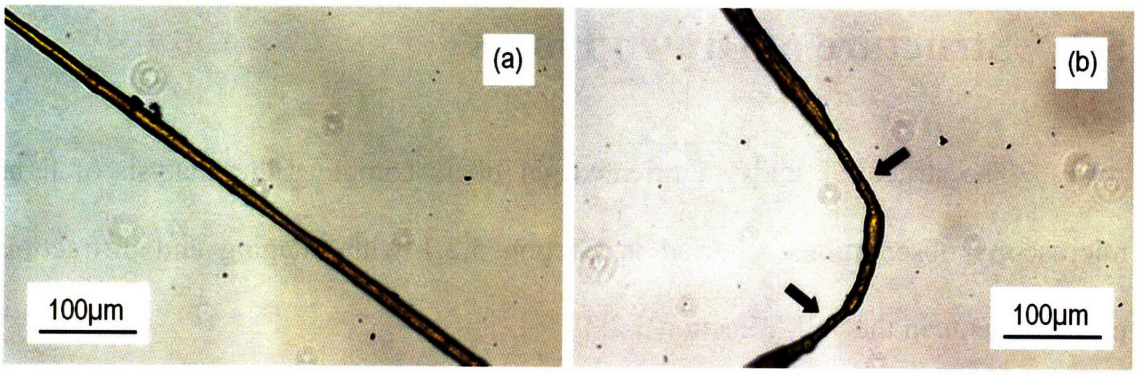

Figure 5-2. (a) Bright-field transmitted light microscopy image of a drawn gel fiber. Fibers were about 15μm in diameter. (b) Two necked regions (arrows) can be observed in this section of the fiber.

Necked regions were analyzed on a light microscope using crossed polars. The maximum intensity of transmitted polarized light is expected after 45° clockwise rotation from the initial configuration illustrated in Figure 5-3-(a). Figures 5-3 (b-c) correspond to 2.5°, 15° and 24.5° clockwise rotations; the LM stage could not rotate up to 45°. The steady increase in intensity observed confirms an anisotropic morphology in the highly oriented necked regions of HFIP-PT gel fibers.

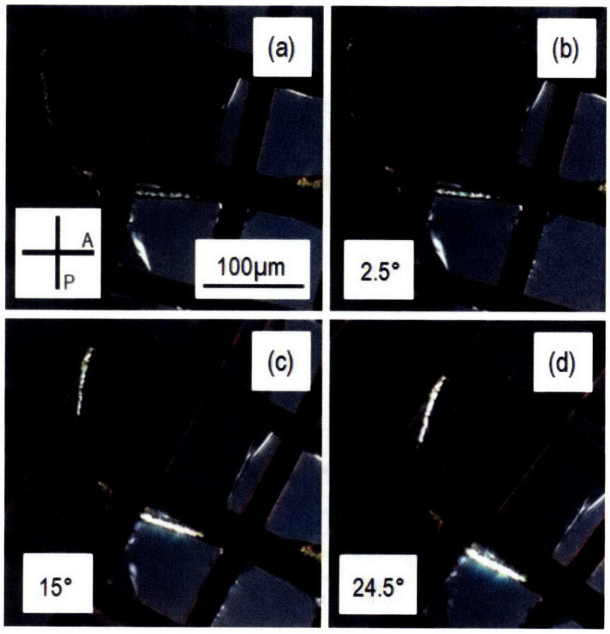

Figure 5-3. Polarized light microscopy analysis of necked regions in an oriented gel fiber. The fiber sits on a carbon film which itself is on a TEM grid. The microscope stage is rotated clockwise from (a) to (d). The strong increase in intensity of transmitted polarized light is representative of a high alignment of chains induced by the necking process. The amount of rotation is indicated in degrees in the lower-left corner (b-d).

5.2.2 Transmission Electron Microscopy

The structural study of drawn gel fibers was further pursued by means of TEM analysis. Although electrons are not transmitted through carbonaceous samples 15µm in thickness, optimal regions were found at the ends of fiber segments and in peeled off regions, i.e. thin segments that come off the fiber.

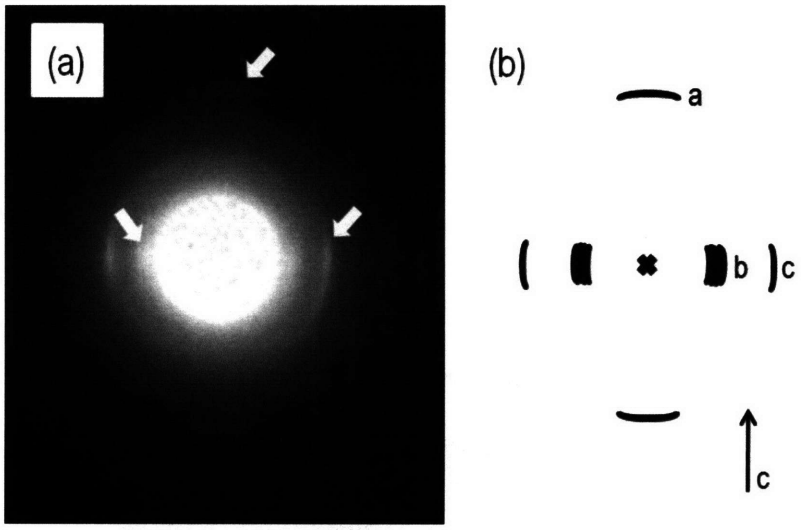

Figure 5-4. (a) Electron diffraction pattern of an oriented region in an HFIP-PT gel fiber. The arrows point towards the three sets of reflections observed; d-spacings are reported in Table 5-1. The contrast has been digitally enhanced. This type of diffraction pattern geometry, with reflections along the equatorial and meridional directions, coincides with the electron diffraction pattern of oriented gel films, see Figure 4-8.

Figure 5-4 shows an electron diffraction pattern obtained from a region located at the end of a fiber segment. There are additional higher order peaks along the equatorial compared to electron diffraction patterns observed on oriented gel films (see Figure 4-8). The reflection along the meridional (labeled a) in Figure 5-4 corresponds to a spacing of 0.26nm in direct space, 0.61nm and 0.39nm spacings are calculated for the inner and outer equatorial reflections (labeled b and c

respectively). These spacings differ from those calculated previously based on electron diffraction measurements on oriented gel films as illustrated in Table 5-1.

Table 5-1. Comparative of d-spacings calculated from reflections observed in the electron diffraction patterns of oriented gel films and fibers.

Reflections	Observed Spacings (nm)	
	Films	Fibers
a	0.12	0.26
b	0.42	0.61
c	0.21-0.24	0.39

Figure 5-5-(a) illustrates the region contributing to the diffraction pattern in Figure 5-4. A lower magnification micrograph, see Figure 5-5-(b), illustrates how the support film bends due to the weight of the fiber. The region could probably be offset with respect to the eucentric plane which could contribute to the disparity of spacings between electron diffraction measurements on oriented films and fibers. Other factors that could contribute to having different spacings are a difference in gel composition (wt% solvent), which could affect chain packing, or the possibility that the gel could display polymorphism with formation of a different crystalline structure.

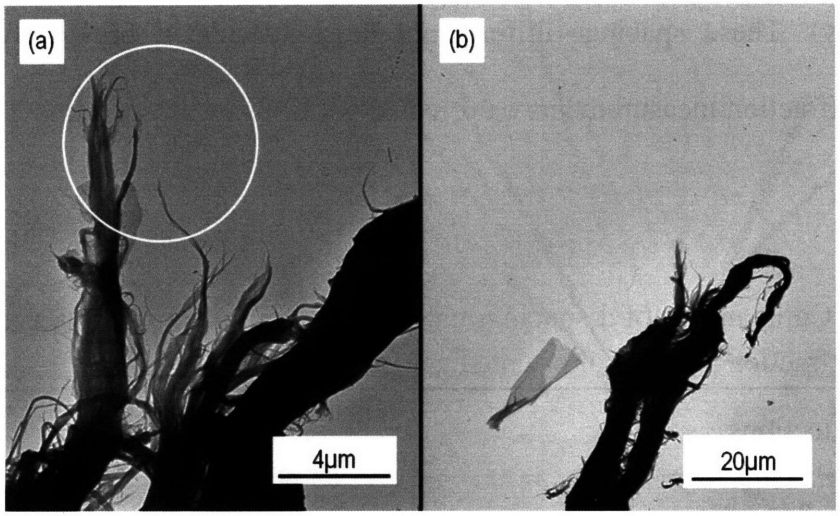

Figure 5-5. Bright-field TEM micrographs corresponding to the end of an oriented fiber segment. (a) The white circle illustrates the region contributing to the diffraction pattern in Figure 5-4. (b) Bright-field electron micrograph illustrating the formation of wrinkles on the carbon film support as a result of bending produced by the weight of the fiber.

The geometry of diffraction patterns observed in oriented fibers is similar to the one observed in oriented films with main reflections distributed along the meridional and equatorial directions. The meridional direction correspond to the direction along the fiber axis suggesting a similar arrangement of HFIP-PT chains as in oriented gel films, see Figure 4-8.

5.3 Chapter Conclusions

Based on a similar protocol followed during thin film preparation, namely melting the gel and mechanically deforming the gel during cool-down, the preparation of drawn fibers demonstrates that those regions in HFIP-PT gels under high stress field such as necked regions, can result in high degree of chain orientation. Based on the similarity in electron diffraction pattern geometry, we suggest the structure of HFIP-PT drawn fibers follows the anisotropic morphology found in shear oriented thin films. The disparity in spacing with regard to the measurement on oriented gel films could arise from a geometrical factor due to bending of sample supporting film in the TEM grid, a difference in gel composition or to polymorphism.

Chapter 6

Conclusions and Future Directions

While the addition of lateral pendant groups enhances solubility and facilitates processing of conjugated polymers, strategies limited to solution processing, i.e. dissolution of the polymer and casting into thin films via solvent evaporation, present poor compounding flexibility such as for the homogeneous incorporation of additives through mixing, e.g. dopants, and relatively poor control over sample morphology. In this work, we employed a gelation strategy to incorporate significant plasticity into conjugated polymer materials. A plastic gel route is proposed for processing highly oriented conjugated polymer films and fibers.

In Section 6.1, we review the main results of this thesis, namely the gelation mechanism of HFIP-PT and the structural characterization of highly oriented gel films and fibers. Finally, Section 6.2 points out possible directions for future work.

6.1 A Plastic Gel Route for Conjugated Polymers

The incorporation of HFIP pendant groups to PT makes the polymer readily soluble in common solvents such as THF. In addition to enhanced solubility, HFIP introduces the possibility for significant hydrogen bond forming capabilities of the polymer. We observed that HFIP-PT is able to build an isotropic self-supporting network structure. In Chapter 3, we propose a gelation mechanism based upon a combination of polymer-polymer chain interactions and interchain hydrogen bonding associations through HFIP pendant groups promoted by addition of small nonsolvent polar protic molecules such as methanol and water to a HFIP-PT/THF solution. The reversibility of these physical crosslinks incorporates the ability to melt the gel and to plastically deform the gel.

The gel network can be melted and then transformed mechanically to form anisotropic morphologies with the chains aligned along the tensile direction as reported in Chapter 4 and 5. Key to attaining highly oriented films and fibers is to mechanically deform the material during the reformation transition from the molten state to the gel state upon cool-down. The high degree of anisotropy is confirmed by dichroism analysis of oriented gel films. Based on electron and x-ray diffraction studies, we suggest the uniaxially oriented gel morphology comprises an anisotropic distribution of tie points in the form of ordered clusters in an overall swollen network. In these crystalline regions, conjugated backbones are π-stacked with

respect to each other neighbors and lie parallel to the substrate, as illustrated in Figure 4-8.

The build-up of a network of linkages based on chain-chain interactions and hydrogen bonding associations between HFIP groups and small polar protic molecules during gel reformation from the molten state is necessary for stress transmission during film and fiber processing. Jointly with the rigid nature of HFIP-PT chains and the proximity of the hydroxyl group in HFIP to the PT backbone, these reversible linkages allow chains to align upon mechanical deformation. The mechanically induced structural rearrangement from an isotropic to an anisotropic conjugated polymer gel occurs when transitioning from the molten to the gel state. However, the lack of HFIP-PT regioregularity is a limiting factor to achieve a full crystallographic registry between π-stacked chains and to attain an overall highly ordered structure except in the most densely packed clusters.

6.2 Suggestions for Future Work

In Chapter 1, we envisioned the ideal anisotropic conjugated polymer morphology would consist of a three-dimensional network with uniaxial orientation of the conjugated backbones in a continuous single crystal-like morphology. The findings gathered over the course of this thesis suggest the incorporation of strong

dipolar functionalities to rigid conjugated backbones enables gelation leading to a processing technology with high control over microstructure and a potential for high compounding versatility. A complete gel processing route toward thermally stable and highly oriented conjugated polymer films and fibers could benefit from the combination of the following 4 basic processes: Gelation, compounding (e.g. doping), mechanical deformation and crosslinking.

A conjugated polymer plastic gel has the potential to combine several positive aspects that could make it attractive from a materials design standpoint. Appropriate gelling agents could perform further functions such as doping or interchain covalent crosslinking via chemical coupling in addition to gel formation via reversible physical crosslinks. The ability to melt the gel could lead to a uniform mixing of conjugated polymers with dopants and/or other additives. Mechanical deformation during film and fiber drawing is a macroscopic input with an output (orientation) at the molecular level which could be important from a practical viewpoint, e.g. for fabrication of large areas and high sample throughput. Furthermore, the possibility to prepare free-standing films could be a substrate-free process to impart a high degree of chain orientation in conjugated polymer films.

The detailed list of suggestions for future work follows:

1. The strong dipolar functionality incorporated into PT backbones through HFIP pendant groups could be extended to other conjugated polymers such as those illustrated in Figure 2-1.

2. The possibility to synthesize HFIP-PT via a regioselective pathway could improve polymer regioregularity. Higher molecular regularity could facilitate improved crystallization of the pristine polymer allowing a better order, a better crystallographic analysis and most importantly improved charge transport properties. The detailed knowledge of the unit cell dimensions and chain packing of HFIP-PT could help in more complete structural characterization of the material, in particular of the crystalline phases. Furthermore, higher regioregularity could improve molecular registry between π-stacked chains which could translate in better chain-chain interactions and delocalization of electron wavefunction with positive effect on charge carrier mobility.

3. The gelling agent could perform the additional function of dopant molecule. In this scenario, gelation and doping could take place simultaneously in a dopant solution.

4. Crosslinking the anisotropic gel via chemical coupling could generate a covalent three-dimensional network with better thermal stability and improved ability to retain dopant molecules. The choice of gelling

agent would then require a molecule able to induce physical gelation and permit further covalent crosslinking. We suggest dicarboxilic acids could be suitable candidates to perform this task, see Figure 6-1. The transformation into a covalent network could take place via chemical coupling between HFIP pendant groups and gelling molecules through esterification reactions. We also suggest an exploratory study of alternative crosslinking agents to avoid the potential negative effect of byproducts such as water.

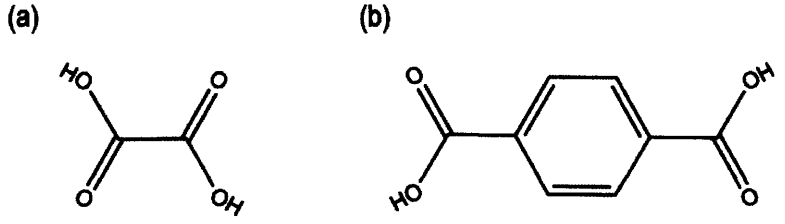

Figure 6-1. Chemical structures of (a) Oxalic acid and (b) Terephthalic acid.

In addition to solvent interdiffusion employed in this work, alternative gelation protocols could be considered. For example, mixing different solutions, e.g. polymer/THF and gelling agent/THF, could enable a better control of gel composition and allow a wider range of gelling

molecules to be considered. The degree of covalent crosslinking could be evaluated in isotropic gels by means of dynamic scanning calorimetry or mechanical characterization. In anisotropic morphologies, the effect of covalent crosslinking could be quantified via the thermal stability of optical anisotropy as illustrated in Chapter 4..

5. The optimal composition polymer/gelling agent is expected to depend on the balance between gelation, plasticity and chain packing. A minimal concentration of gelling agent able to induce gelation and plasticity could favor better chain packing. XRD could be used to evaluate the impact of gelling agent content on chain packing in oriented gels.

6. Future work could employ cryo-TEM techniques to investigate the detailed structural analysis of isotropic and anisotropic HFIP-PT gels. New insights could provide a better understanding of the transition mechanism between isotropic and anisotropic gel morphologies upon mechanical orientation. Moreover, the possibility to draw self-supporting films could enable XRD analysis in transmission and access complementary structural information. Assuming it is possible to prepare oriented films able to withstand under the electron beam enough time to provide a workable diffraction pattern, we suggest the use of dark-field imaging in the TEM to attempt mapping the distribution of crystalline-

amorphous regions in order to quantify the density of the crystal/amorphous interfaces and the fraction of crystal/amorphous domains.

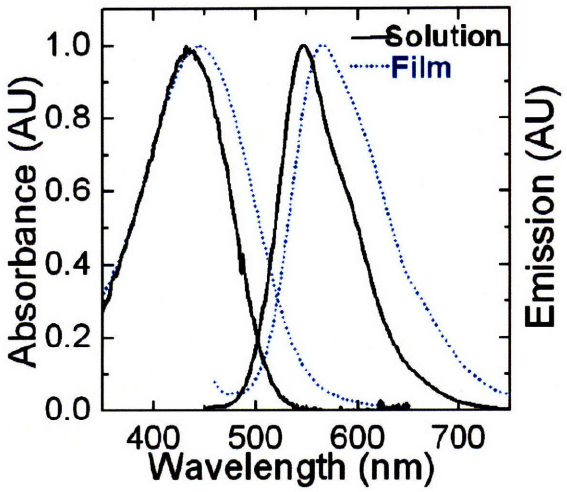

Figure 6-2. UV-VIS absorption and fluorescence emission spectra of HFIP-PT in chloroform solution (solid lines) and thin films of HFIP-PT spin-coated from THF solution (dotted lines). Reproduced from Ref. [71].

7. Optical absorption is typically used to analyze the conformational disorder in thin films. In an earlier study, Wang et al. reported the UV-VIS absorption and fluorescence emission of HFIP-PT on solution (chloroform) and thin films of HFIP-PT spin-coated from THF

solution,[79] see Figure 6-2. UV-VIS absorption of oriented gel films could complement this study. A more planar backbone has a longer absorption and the width of the peak can qualitatively be used as an indication of the uniformity of the conformation.

8. The ability to melt HFIP-PT gels could motivate exploring a general pathway for conjugated polymer compounding. In the molten state, the gel could be like a syrup whose viscosity is expected to be temperature dependent. Enhanced mixing could yield a good dispersion and homogeneity of additives.

9. Applications:

9.1. Of interest could be to prepare self-supporting films. Highly oriented conjugated polymer films could be incorporated in multilayer device architectures such as transistors or light-emitting diodes.

9.2. In general, due to facile access of new components into the gel a swollen conjugated polymer network could facilitate counterions transport during swelling/de-swelling cycles in artificial muscles or analyte diffusion in sensing applications.

9.3. Covalent coupling of conjugated polymer backbones through hydroxyl moieties could be relevant to develop composites based on compounding conjugated polymer gels with functionalized CNT's[80] or other graphitic allotropes. The melted gel could facilitate uniform mixing and the ability to mechanically orient the gel could lead to anisotropic composite materials with enhanced mechanical and charge transport properties.

The mechanism by which a dipole functionalized polythiophene can form a reversible network able to be deformed into structurally oriented films and fibers appears to be of interest in the development of novel processing routes for conjugated polymers. This study highlights the versatility of incorporating plasticity in the design of conjugated polymer materials via a gel processing technology and its potential for applications.

References

[1] Forrest, Stephen R. The path to ubiquitous and low-cost organic electronic appliances on plastic. Nature (London, United Kingdom) (2004), 428(6986), 911-918.

[2] Muthukumar, M.; Ober, C. K.; Thomas, E. L.. Competing interactions and levels of ordering in self-organizing polymeric materials. Science (Washington, D. C.) (1997), 277(5330), 1225-1232.

[3] Cohen, Yachin; Saruyama, Yasuo; Thomas, Edwin L. Crystal solvates in the poly[p-phenylene(benzo[1,2-d:4,5-d']bisthiazole-2,6-diyl)]/poly(phosphoric acid)/water system. Macromolecules (1991), 24(5), 1161-7.

[4] Handbook of Conducting Polymers (2007) Skotheim, Terje A.; Reynolds, John R. (Eds) CRC Press LLC, Boca Raton, FL, USA.

[5] Handbook of Oligo- and Polythiophenes (1999) Fichou, Denis (Ed.) Wiley-VCH Verlag GmbH, Weinheim, Germany.

[6] Shirakawa, Hideki; Louis, Edwin J.; MacDiarmid, Alan G.; Chiang, Chwan K.; Heeger, Alan J. Synthesis of electrically conducting organic polymers: halogen derivatives of polyacetylene, (CH)x. Journal of the Chemical Society, Chemical Communications (1977), (16), 578-80.

[7] Naarmann, H.; Theophilou, N. New process for the production of metal-like, stable polyacetylene. Synthetic Metals (1987), 22(1), 1-8.

[8] Kittel, C. Introduction to Solid State Physics (1986) Wiley.

[9] Heeger, A. J.; Kivelson, S.; Schrieffer, J. R.; Su, W. P. Solitons in conducting polymers. Reviews of Modern Physics (1988), 60(3), 781-850.

[10] Horowitz, G.; Delannoy, P. Charge transport in semiconducting oligothiophenes. Handbook of Oligo- and Polythiophenes (1999), 283-316. Fichou, Denis (Ed.) Wiley-VCH Verlag GmbH, Weinheim, Germany.

[11] Wang, Z. H.; Li, C.; Scherr, E. M.; MacDiarmid, A. G.; Epstein, A. J. Three dimensionality of "metallic" states in conducting polymers: polyaniline. Physical Review Letters (1991), 66(13), 1745-8.

[12] Fincher, C. R., Jr.; Peebles, D. L.; Heeger, A. J.; Druy, M. A.; Matsumura, Y.; MacDiarmid, A. G.; Shirakawa, H.; Ikeda, S. Anisotropic optical properties of pure and doped polyacetylene. Solid State Communications (1978), 27(5), 489-94.

[13] Cao, Yong; Smith, Paul; Heeger, Alan J. Mechanical and electrical properties of polyacetylene films oriented by tensile drawing. Polymer (1991), 32(7), 1210-18.

[14] Nalwa, H. S. (Ed.) Handbook of Organic Conductive Molecules and Polymers, Volume 3: Conductive Polymers: Spectroscopy and Physical Properties. Mohammad, F. Chapter 16: Degradation and Stability of Conductive Polymers, Wiley (1997).

[15] Wang, Yading; Rubner, M. F.; Buckley, L. J. Stability studies of electrically conducting polyheterocycles. Synthetic Metals (1991), 41(3), 1103-8.

[16] Wang, Yading; Rubner, M. F. Stability studies of the electrical conductivity of various poly(3-alkylthiophenes). Synthetic Metals (1990), 39(2), 153-75.

[17] Loponen, M. T.; Taka, T.; Laakso, J.; Vakiparta, K.; Suuronen, K.; Valkeinen, P.; Osterholm, J. E. Doping and dedoping processes in poly(3-alkylthiophenes). Synthetic Metals (1991), 41(1-2), 479-84.

[18] Li, Ling; Collard, David M. Tuning the Electronic Structure of Conjugated Polymers with Fluoroalkyl Substitution: Alternating Alkyl/Perfluoroalkyl-Substituted Polythiophene. Macromolecules (2005), 38(2), 372-378.

[19] Yamamoto, Takakazu; Morita, Atsushi; Miyazaki, Yuichi; Maruyama, Tsukasa; Wakayama, Hiroshi; Zhou, Zhen Hua; Nakamura, Yoshiyuki; Kanbara, Takaki; Sasaki, Shintaro; Kubota, Kenji. Preparation of conjugated poly(thiophene-2,5-diyl), poly(p-phenylene), and related polymers using zerovalent nickel complexes. Linear structure and properties of the □ -conjugated polymers. Macromolecules (1992), 25(4), 1214-23.

[20] Elsenbaumer, R. L.; Jen, K. Y.; Oboodi, R. Processible and environmentally stable conducting polymers. Synthetic Metals (1986), 15(2-3), 169-74.

[21] Odian, G. Principles of Polymerization (2004) Wiley.

[22] McCullough, Richard D. The chemistry of conducting polythiophenes. Advanced Materials (Weinheim, Germany) (1998), 10(2), 93-116.

[23] Patil, A. O.; Heeger, A. J.; Wudl, Fred. Optical properties of conducting polymers. Chemical Reviews (Washington, DC, United States) (1988), 88(1), 183-200.

[24] Chen, Tian-An; Wu, Xiaoming; Rieke, Reuben D. Regiocontrolled Synthesis of Poly(3-alkylthiophenes) Mediated by Rieke Zinc: Their Characterization and Solid-State Properties. Journal of the American Chemical Society (1995), 117(1), 233-44.

[25] Bouman, Michiel M.; Meijer, E.W. Stereomutation in optically active regioregular polythiophenes. Advanced Materials (Weinheim, Germany) (1995), 7(4), 385-7.

[26] Materials Science and Technology. R. W. Cahn, P. Haasen, E. J. Kramer (Eds). Vol. 12, Structure and Properties of Polymers. Thomas, E. L. (Ed.). (1993) VCH

[27] McCullough, Richard D.; Lowe, Renae D. Enhanced electrical conductivity in regioselectively synthesized poly(3-alkylthiophenes). Journal of the Chemical Society, Chemical Communications (1992), (1), 70-2.

[28] Forrest, Stephen R. The path to ubiquitous and low-cost organic electronic appliances on plastic. Nature (London, United Kingdom) (2004), 428(6986), 911-918.

[29] H. Sirringhaus. Device physics of solution-processed organic field-effect transistors. *Advanced Materials*. 17, 2411 (2005).

[30] Jiang, X.; Harima, Y.; Yamashita, K.; Tada, Y.; Ohshita, J.; Kunai, A. A transport study of poly(3-hexylthiophene) films with different regioregularities. Synthetic Metals (2003), 135-136 351-352.

[31] Kline, R. Joseph; McGehee, Michael D.; Kadnikova, Ekaterina N.; Liu, Jinsong; Frechet, Jean M. J. Controlling the field-effect mobility of regioregular polythiophene by changing the molecular weight. Advanced Materials (Weinheim, Germany) (2003), 15(18), 1519-1522.

[32] Fichou, Denis; Ziegler, Christiane. Structure and properties of oligothiophenes in the solid state: single crystals and thin films. Handbook of Oligo- and Polythiophenes (1999), 183-282.

[33] Horowitz, Gilles; Bachet, Bernard; Yassar, Abderrahim; Lang, Philippe; Demanze, Frederic; Fave, Jean-Louis; Garnier, Francis. Growth and Characterization of Sexithiophene Single Crystals. Chemistry of Materials (1995), 7(7), 1337-41.

[34] Bruckner, Sergio; Porzio, William. The structure of neutral polythiophene: an application of the Rietveld method. Makromolekulare Chemie (1988), 189(4), 961-7.

[35] Prosa, T. J.; Winokur, M. J.; Moulton, Jeff; Smith, Paul; Heeger, A. J. X-ray structural studies of poly(3-alkylthiophenes): an example of an inverse comb. Macromolecules (1992), 25(17), 4364-72.

[36] Brinkmann, Martin; Wittmann, Jean-Claude. Orientation of regioregular poly(3-hexylthiophene) by directional solidification: a simple method to reveal the semicrystalline structure of a conjugated polymer. Advanced Materials (Weinheim, Germany) (2006), 18(7), 860-863.

[37] Sirringhaus, H.; Brown, P. J.; Friend, R. H.; Nielsen, M. M.; Bechgaard, K.; Langeveld-Voss, B. M. W.; Spiering, A. J. H.; Janssen, R. A. J.; Meijer, E. W.; Herwig, P.; De Leeuw, D. M. Two-dimensional charge transport in self-organized, high-mobility conjugated polymers. Nature (London) (1999), 401(6754), 685-688.

[38] Wang, Guangming; Swensen, James; Moses, Daniel; Heeger, Alan J. Increased mobility from regioregular poly(3-hexylthiophene) field-effect transistors. Journal of Applied Physics (2003), 93(10, Pt. 1), 6137-6141.

[39] Kim, Do Hwan; Park, Yeong Don; Jang, Yunseok; Yang, Hoichang; Kim, Yong Hoon; Han, Jeong In; Moon, Dae Gyu; Park, Soojin; Chang, Taihyun; Chang, Changhwan; Joo, Mankil; Ryu, Chang Y.; Cho, Kilwon. Enhancement of field-effect mobility due to surface-mediated molecular ordering in regioregular polythiophene thin film transistors. Advanced Functional Materials (2005), 15(1), 77-82.

[40] A. Andreatta, P. Smith. Processing of conductive polyaniline-UHMW polyethylene blends from solutions in nonpolar solvents. Synthetic Metals. 55, 1017 (1993).

[41] A. Montali, C. Bastiaansen, P. Smith, C. Weder. Polarizing energy transfer in photoluminescent materials for display applications. Nature. 392, 261 (1998).

[42] Wittmann, J. C.; Lotz, B.. Epitaxial crystallization of polymers on organic and polymeric substrates. Progress in Polymer Science (1990), 15(6), 909-48.

[43] Wittmann, J. C.; Lotz, B.; Smith, P. Formation of highly oriented films by epitaxial crystallization on polymeric substrates. Progress in Colloid & Polymer Science (1993), 92(Orientational Phenomena in Polymers), 32-8.

[44] A. Thierry, C. Mathieu, C. Straupe, J. C. Wittmann, B. Lotz, V. Da Costa, J. Le Moigne. Polymer and organic molecules ordered via epitaxy: geometrical and molecular interactions. Macromolecular Symposia. 166, 43 (2001).

[45] M. Grell, W. Knoll, D. Lupo, A. Meisel, T. Miteva, D. Neher, H. G. Nothofer, U. Scherf, A. Yasuda. Blue Polarized Electroluminescence from a Liquid Crystalline Polyfluorene. Advanced Materials. 11, 671 (1999).

[46] Sakamoto, Kenji; Usami, Kiyoaki; Uehara, Yoichi; Ushioda, Sukekatsu. Excellent uniaxial alignment of poly(9,9-dioctylfluorenyl-2,7-diyl) induced by photoaligned polyimide films. Applied Physics Letters. 87, 211910 (2005).

[47] Patel, J. S.; Lee, Sin Doo; Baker, G. L.; Shelburne, J. A., III. Epitaxial growth of aligned polydiacetylene films on anisotropic orienting polymers. Applied Physics Letters (1990), 56(2), 131-3.

[48] Kanetake, Tatsuo; Ishikawa, Ken; Koda, Takao; Tokura, Yoshinori; Takeda, Kenji. Highly oriented polydiacetylene films by vacuum deposition. Applied Physics Letters (1987), 51(23), 1957-9.

[49] M. Hamaguchi, K. Yoshino. Polarized electroluminescence from rubbing-aligned poly(2,5-dinonyloxy-1,4-phenylenevinylene) films. Applied Physics Letters. 67, 3381 (1995).

[50] Yang, C. Y.; Soci, C.; Moses, D.; Heeger, A. J. Aligned rrP3HT film: Structural order and transport properties. Synthetic Metals (2005), 155(3), 639-642.

[51] V. Cimrova, M. Remmers, D. Neher, G. Wegner. Polarized Light Emission from LEDs Prepared by the Langmuir-Blodgett Technique. Advanced Materials. 8, 146 (1996).

[52] Cao, Yong; Smith, Paul; Heeger, Alan J. Mechanical and electrical properties of polyacetylene films oriented by tensile drawing. Polymer (1991), 32(7), 1210-18.

[53] Dyreklev, Peter; Berggren, Magnus; Inganaes, Olle; Andersson, Mats R.; Wennerstroem, Olof; Hjertberg, Thomas. Polarized electroluminescence from an oriented substituted polyhiophene in a light emitting diode. Advanced Materials (Weinheim, Germany) (1995), 7(1), 43-5.

[54] Kaneto, K.; Yoshino, K. Optical anisotropy of polythiophene films. Synthetic Metals (1989), 28(1-2), C287-C292.

[55] Pytel, Rachel; Thomas, Edwin; Hunter, Ian. Anisotropy of Electroactive Strain in Highly Stretched Polypyrrole Actuators. Chemistry of Materials (2006), 18(4), 861-863.

[56] Albalak, Ramon J.; Thomas, Edwin L. Microphase separation of block copolymer solutions in a flow field. Journal of Polymer Science, Part B: Polymer Physics (1993), 31(1), 37-46.

[57] Breen, Craig A.; Deng, Tao; Breiner, Thomas; Thomas, Edwin L.; Swager, Timothy M. Polarized Photoluminescence from Poly(p-phenylene-ethynylene) via a Block Copolymer Nanotemplate. Journal of the American Chemical Society (2003), 125(33), 9942-9943.

[58] Gu, Hongwei; Zheng, Rongkun; Zhang, Xixiang; Xu, Bing. Using soft lithography to pattern highly oriented polyacetylene (HOPA) films via solventless polymerization. Advanced Materials (Weinheim, Germany) (2004), 16(15), 1356-1359.

[59] Hu, Zhijun; Muls, Benoit; Gence, Loiek; Serban, Dana A.; Hofkens, Johan; Melinte, Sorin; Nysten, Bernard; Demoustier-Champagne, Sophie; Jonas, Alain M. High-Throughput Fabrication of Organic Nanowire Devices with Preferential Internal Alignment and Improved Performance. Nano Letters (2007), 7(12), 3639-3644.

[60] Z. Zheng, K. H. Yim, M. S. M. Saifullah, M. E. Welland, R. H. Friend, J. S. Kim, W. T. S. Huck. Uniaxial alignment of liquid-crystalline conjugated polymers by nanoconfinement. Nano Letters. 7, 987 (2007).

[61] Wittmann, Jean Claude; Smith, Paul. Highly oriented thin films of poly(tetrafluoroethylene) as a substrate for oriented growth of materials. Nature (London, United Kingdom) (1991), 352(6334), 414-17.

[62] M. Misaki, Y. Ueda, S. Nagamatsu, Y. Yoshida, N. Tanigaki, K. Yase. Formation of single-crystal-like poly(9,9-dioctylfluorene) thin film by the friction-transfer technique with subsequent thermal treatments. Macromolecules. 37, 6926 (2004).

[63] Hoogboom, Johan; Swager, Timothy M. Increased Alignment of Electronic Polymers in Liquid Crystals via Hydrogen Bonding Extension. Journal of the American Chemical Society (2006), 128(47), 15058-15059.

[64] Y. Kubo, Y. Kitada, R. Wakabayashi, T. Kishida, M. Ayabe, K. Kaneko, M. Takeuchi, S. Shinkai. A supramolecular bundling approach toward the alignment of conjugated polymers. Angewandte Chemie, International Edition. 45, 1548 (2006).

[65] Edwards, John H.; Feast, W. James., A new synthesis of poly(acetylene). Polymer (1980), 21(6), 595-6.

[66] Granier, Thierry; Thomas, Edwin L.; Gagnon, David R.; Karasz, Frank E.; Lenz, Robert W. Structure investigation of poly(p-phenylene vinylene). Journal of Polymer Science, Part B: Polymer Physics (1986), 24(12), 2793-804.

[67] Wittmann, J. C.; Manley, R. St. John. Polymer-monomer binary mixtures. I. Eutectic and epitaxial crystallization in poly(caprolactone)-trioxane mixtures. Journal of Polymer Science, Polymer Physics Edition (1977), 15(6), 1089-100.

[68] De Rosa, Claudio; Park, Cheolmin; Thomas, Edwin L.; Lotz, Bernard. Microdomain patterns from directional eutectic solidification and epitaxy. Nature (London) (2000), 405(6785), 433-437.

[69] Muthukumar, M.; Ober, C. K.; Thomas, E. L.. Competing interactions and levels of ordering in self-organizing polymeric materials. Science (Washington, D. C.) (1997), 277(5330), 1225-1232.

[70] Amara, J. P.; Swager, T. M. Synthesis and Properties of Poly(phenylene ethynylene)s with Pendant Hexafluoro-2-propanol Groups. *Macromolecules* **2005**, *38*, 9091.

[71] Wang, F.; Gu, H.; Swager, T. M. Carbon Nanotube/Polythiophene Chemiresistive Sensors for Chemical Warfare Agents. *J. Am. Chem. Soc.* **2008**, *130*, 5392.

[72] From Ref. [71]: After HFIP-PT was polymerized with anhydrous iron trichloride in chloroform, the mixture was diluted with tetrahydrofuran, reduced with sodium thiosulphate, then washed sequentially with water, hydrazine aqueous solution, water, brine, dried over MgSO4, filtered with a 0.2 μm PTFE filter and partially evaporated under reduced pressure. The polymer solution was then precipitated into hexane. The precipitate was isolated by centrifugation and decantation of the liquid. The precipitate was dissolved in tetrahydrofuran and precipitated into hexane again.

The precipitation was repeated once more. The material was dried under vacuum to yield an orange-red solid.

[73] Encyclopedia of Analytical Chemistry. R. A. Meyers (Ed.). John Wiley & Sons Ltd, **2000**.

[74] The Aldrich Library of FT-IR spectra. Pouchert, C. J. Aldrich Chemical Company **1985**.

[75] Estimate based upon Nam et al. Journal of Applied Polymer Science (2008), 107(3), 1547-1554). After 24h at less than 30Torr and room temperature the amount of HFIP released in gelatin based fibers decreased from 114ppm to 14ppm, a factor of 8.

[76] Prosa, T. J.; Winokur, M. J.; Moulton, J.; Smith, P.; Heeger, A. J. X-ray structural studies of poly(3-alkylthiophenes): an example of an inverse comb. *Macromolecules* **1992**, *25*, 4364.

[77] Papkov, S. P. Liquid crystalline order in solutions of rigid-chain polymers. *Adv. Polym. Sci.* **1984**, *59*, 75.

[78] (a) Cohen, Y.; Thomas, E. L. Microfibrillar network of a rigid rod polymer. 1. Visualization by electron microscopy. *Macromolecules* **1988**, *21*, 433. (b) Cohen, Y.; Thomas, E. L. Microfibrillar network of a rigid rod polymer. 2. Small-angle x-ray scattering. *Macromolecules* **1988**, *21*, 436.

[79] Wang, F.; Gu, H.; Swager, T. M. Carbon Nanotube/Polythiophene Chemiresistive Sensors for Chemical Warfare Agents. *J. Am. Chem. Soc.* 2008, 130, 5392.

[80] Zhang, Wei; Swager, Timothy M. Functionalization of Single-Walled Carbon Nanotubes and Fullerenes via a Dimethyl Acetylenedicarboxylate-4-Dimethylaminopyridine Zwitterion Approach. Journal of the American Chemical Society (2007), 129(25), 7714-7715.